AD-A142 435 PROTON-INDUCED SINGLE EVENT UPSETS IN 71 EARTH-SATELLITE ENVIRONMENTS(U) NAVAL RESEARCH LAB WASHINGTON DC W L BENDEL 14 JUN 84 NRL-MR-5364

1/1

UNCLASSIFIED F/G 9/2 NL

END
DATE
FILMED
8 84
DTIC

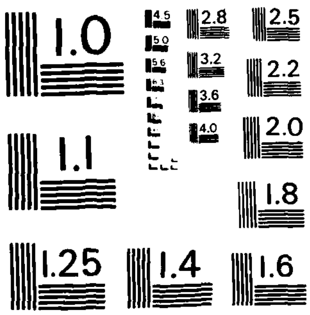

MICROCOPY RESOLUTION TEST CHART
NATIONAL BUREAU OF STANDARDS-1963-A

AD-A142 435

AD-A142435

SECURITY CLASSIFICATION OF THIS PAGE

REPORT DOCUMENTATION PAGE

1a REPORT SECURITY CLASSIFICATION
UNCLASSIFIED

1b RESTRICTIVE MARKINGS

2a SECURITY CLASSIFICATION AUTHORITY

2b DECLASSIFICATION/DOWNGRADING SCHEDULE

3 DISTRIBUTION/AVAILABILITY OF REPORT
Approved for public release; distribution unlimited.

4 PERFORMING ORGANIZATION REPORT NUMBER(S)
NRL Memorandum Report 5364

5 MONITORING ORGANIZATION REPORT NUMBER(S)

6a NAME OF PERFORMING ORGANIZATION
Naval Research Laboratory

6b OFFICE SYMBOL (If applicable)
Code 6611

7a NAME OF MONITORING ORGANIZATION

6c ADDRESS (City, State and ZIP Code)
Washington, DC 20375

7b ADDRESS (City, State and ZIP Code)

8a NAME OF FUNDING/SPONSORING ORGANIZATION
DNA and NAVELEX

8b OFFICE SYMBOL (If applicable)

9 PROCUREMENT INSTRUMENT IDENTIFICATION NUMBER

8c ADDRESS (City, State and ZIP Code)
Washington, DC 20305 Washington, DC 20360

10 SOURCE OF FUNDING NOS

PROGRAM ELEMENT NO	PROJECT NO.	TASK NO	WORK UNIT NO
			DN080-229

11 TITLE (Include Security Classification)
(See page ii)

12 PERSONAL AUTHOR(S)
Bendel, W.L.

13a TYPE OF REPORT
Final

13b TIME COVERED
FROM TO

14 DATE OF REPORT (Yr., Mo., Day)
June 14, 1984

15 PAGE COUNT
42

16 SUPPLEMENTARY NOTATION
(See page ii)

17 COSATI CODES

FIELD	GROUP	SUB. GR.

18 SUBJECT TERMS (Continue on reverse if necessary and identify by block number)
Single event upsets

19 ABSTRACT (Continue on reverse if necessary and identify by block number)

Predicted upset rates are presented, as a function of one experimental parameter, for devices in small earth satellites. Contour maps of SEU rate versus circular orbit inclination and altitude allow predictions at 180-1400 km and 27° to 90°. A computer program is listed, permitting the reader to calculate upsets in any proton flux.

deg

20 DISTRIBUTION/AVAILABILITY OF ABSTRACT
UNCLASSIFIED/UNLIMITED X SAME AS RPT ☐ DTIC USERS ☐

21 ABSTRACT SECURITY CLASSIFICATION
UNCLASSIFIED

22a NAME OF RESPONSIBLE INDIVIDUAL
W. L. Bendel

22b TELEPHONE NUMBER (Include Area Code)
(202) 767-3938

22c OFFICE SYMBOL
Code 6611

DD FORM 1473, 83 APR EDITION OF 1 JAN 73 IS OBSOLETE

SECURITY CLASSIFICATION OF THIS PAGE

SECURITY CLASSIFICATION OF THIS PAGE

11. TITLE (Include Security Classification)

Proton-Induced Single Event Upsets in 71 Earth-Satellite Environments

16. SUPPLEMENTARY NOTATION

This work was partially sponsored by the Defense Nuclear Agency under Subtask X99QMXVA, work unit 00018, work unit title "Single Event Program" and by the Naval Electronic Systems Command under the NRL Spacecraft Survivability/Vulnerability Program.

SECURITY CLASSIFICATION OF THIS PAGE

CONTENTS

Tables

Figures

Proton-Induced Single Event Upsets

in 71 Earth-Satellite Environments

Introduction

An important consideration in the miniaturization of electronic components is the phenomenon of single event upset (SEU). This phenomenon is caused by high-energy radiation, and both internal and external sources of radiation have been implicated. These upsets are a current problem in spacecraft random access memories (RAMs). SEUs will become increasingly important because of the trend to smaller components and more complex circuitry, with more bits of memory. The upsets caused by protons will be particularly significant as satellites carrying multi-megabit memories try to operate in the earth's radiation belts.

We have reported[1] a method of predicting proton-induced SEUs in spacecraft RAMs, using an equation based on laboratory experiments. Data on a given device define the single parameter of the equation, which may be considered as a *figure of merit* for the device.[2] In the present report, the treatment of the method is somewhat shortened, but SEU tables are presented for many more orbital environments, within a specified shield. In addition, contour maps and information are presented to permit upset rate predictions in other circular orbits.

If a silicon chip contains any alpha-emitting impurity, a source of SEUs exists. (Surfaces of adjacent materials can also be a source of alphas.) When, for example, radium 226 decays, it emits an alpha particle with 4.78 MeV (million electron volts) of kinetic energy, and the residual nucleus recoils with 0.09 MeV. These particles produce ionization in whatever material they traverse, freeing one electron per 3.6 eV in the case of silicon. This produces 1.35 million electron-hole pairs, or about 0.22 picocoulomb. If this is sufficient to cause an error in a device (for example, change a bit in a computer memory), an SEU occurs.

Single event upsets may be countered by eliminating the sources or by hardening the circuit. Once internally-produced SEUs were recognized, specific ultrapurification procedures aimed at the heavy elements could be introduced. One can often shield against external radiation. In the case of spacecraft circuitry, which is subject to far more intense radiation than earth-bound circuits, massive shielding is out of the question; spacecraft electronics must be insensitive to SEUs. Radiation hardness is pursued by careful design, selection, and testing of all parts. In addition, error-correction capabilities are provided.

Manuscript approved March 30, 1984.

SEUs due to protons are a significant problem in electronic circuitry of earth-orbiting spacecraft. Unlike a heavier ion, mere passage of a proton does not produce sufficient ionization to upset the usual circuits at the present stage of miniaturization. However, a nuclear reaction initiated by a proton can produce sufficient ionization for an upset. The probability of such upsets can be investigated both experimentally and theoretically. These studies can be used to predict upset rates.

Several groups[3-8] have investigated soft errors in RAMs using accelerator protons. The probability of upset increases rapidly as proton kinetic energy increases from about 20 to 100 MeV, then increases more slowly at higher energies. It appears that cross sections monotonically increase with energy. The results are orders-of-magnitude different for unlike RAMs.

The experimental SEU data, supplemented by nuclear theory and data, are used to develop an equation for upset cross section vs. proton energy, E. The equation uses a sensitivity parameter

$$A = \text{apparent threshold.}$$

This equation is then employed with the proton spectra inside spacecraft to calculate SEU rates as a function of orbit and the single experiment-based parameter for the device considered.

Experimental SEU Data

Data on proton-induced SEUs are presented in Fig. 1. The data on National Semiconductors MM5280, Intel C2107B, and Texas Instruments 4044 devices are taken from Refs. 4 and 6. Note that single devices of the same type may differ widely in SEU tests. The protons were obtained as a 158-MeV beam from the Harvard Cyclotron, degraded by passing through matter. Thus, the protons used in the low-energy bombardments were not monoenergetic.

The Motorola MCM 4116AC-20 and Mostek MK 4116J-2 data[3,5] were obtained with the NRL Cyclotron and the Brookhaven Alternating Gradient Synchrotron.

The others, Signetics 8X350 and four Fairchild devices, were tested by the Jet Propulsion Laboratory group[7,8] at a number of radiation facilities. A factor in the scatter of these data is use of different units with the same type number.

Note that SEUs are a function of the experimental set-up as well as the device. One expects results to depend upon operating voltage and orientation relative to the beam. These dependences are observed in the case of heavy ion bombardment.[2]

Nuclear Data and Theory

As shown elsewhere[7,10], the dominant upset mechanism is a function of device sensitivity and proton energy. Some devices can be upset by the ionization in a proton track and are grossly

EXPERIMENTAL S.E.U. CROSS SECTIONS

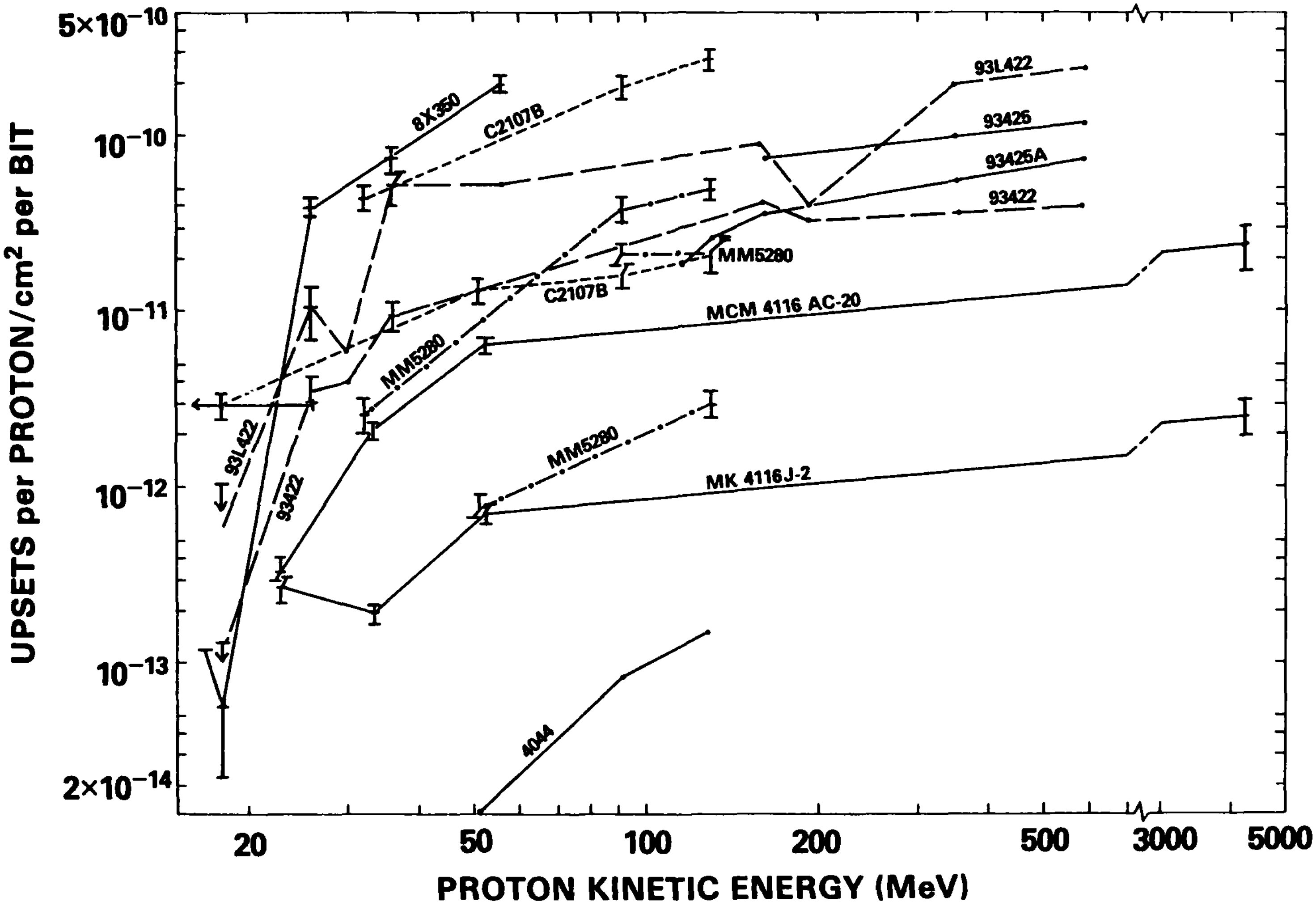

Fig. 1. Experimental upset data with protons of 18 to 4200 MeV.

unfit for spacecraft use. Hence, we should consider only devices unaffected by direct ionization in even the longest track with the funneling effect. A nuclear reaction producing a highly-ionizing track is therefore required for a proton-induced SEU. If a device upsets due to direct ionization, these SEUs are not included here. At the other extreme, proton beams have failed to upset some insensitive devices that are upset by heavy ions.

Nuclear reactions leading to upsets are discussed in Ref. 1. For SEUs due to elastic scattering, the threshold is determined by kinematics. For SEUs due to alpha-producing reactions, the apparent threshold is primarily determined by Coulomb barrier penetration cross sections, not by energy deposition. The shape of the upset cross section, being the sum over these and other reactions, is difficult to estimate, but a cross section that is proportional to $(E - A)^{1.5}$ is reasonable near threshold.[1]

Total proton inelastic cross sections are reviewed by Letaw and coworkers.[11] In the equation which they fit to the data, the cross section approaches a constant value at high energy, being 0.4% less at 1000 MeV than at infinite energy. If the ratio of upset-producing cross section to total inelastic cross section is independent of the energy - a reasonable relationship at high energy - the SEU yield also will be essentially constant at high energy. This is consistent with the SEU data.

Semi-Empirical Equation

Experimental data on SEUs will not show the "true" threshold but will indicate an energy at which the cross section becomes immeasurably small. Therefore, our equation uses a sensitivity parameter, A, called the *apparent threshold*.

The experimental upset cross sections are fitted to a form which is constant at high proton energy, decreasing below about 1000 MeV. The data above 90 MeV are amenable to an exponential dependence upon energy. The lower energy data, as well, fit the form

$$X = X_o\,[1 - \exp(-hY^m)]^n, \qquad (1)$$

where X_o is the limiting cross section. Here, h is a constant and Y is a linear function of energy which, by definition, goes to zero at E = A.

The function Y may be obtained from (E - A) or (E/A - 1). Each choice has some merit; we employ the normalized compromise relationship

$$Y = (18/A)^{0.5}\,(E - A), \qquad (2)$$

with E and A in MeV, here and in Eq. (3). The equation adopted is

$$X = (24/A)^{14}\,[1 - \exp(-0.18\,Y^{0.5})]^4 \qquad (3)$$

in units of 10^{-12} upsets per proton/cm^2 per bit. This equation is plotted in Fig. 2 for various values of A. It fits the data

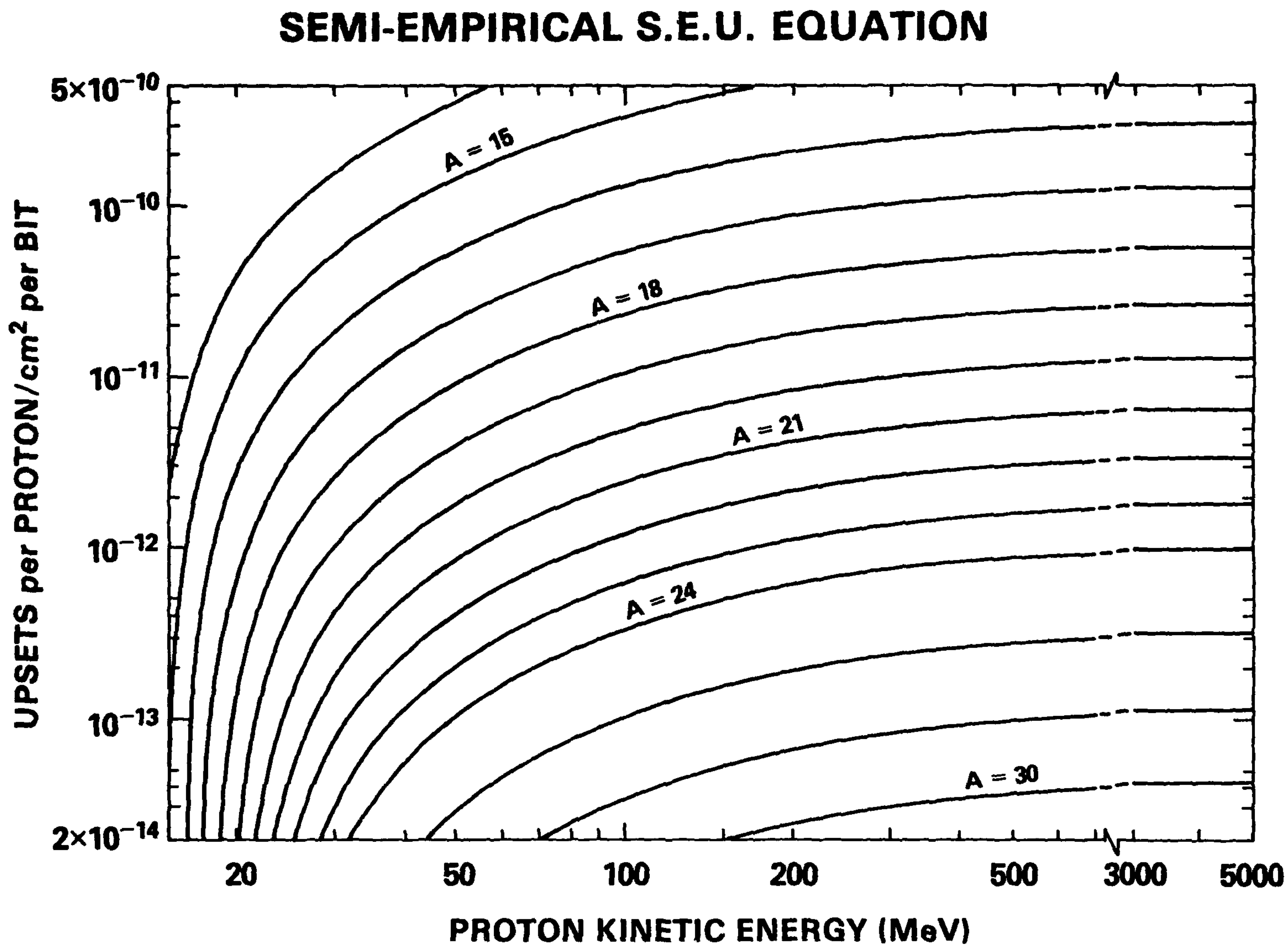

Fig. 2. Upset cross sections using Eq. (3).

quite adequately, although a larger value of mn fits a little better. The value of X is proportional to $(E - A)^2$ at $E = A$, but the average power is 1.5 between, for example, Y = 5 and 17.

If more consistent SEU data were available, a better empirical relationship could be developed. Data near threshold are particularly needed. It does not appear to be feasible, either scientifically or in cost effectiveness, to experimentally determine the fine structure. For a given device, one expects the SEU rate due to one reaction to rise rapidly (on a logarithmic scale) and then flatten. New rises would occur when new reactions or different parts of the circuit begin to produce a significant number of upsets.

We have determined a value of A for each device used here. Some data were given lesser weight and measurements within 4 MeV of A were ignored. The ratios of measured SEU cross sections to X(E,A) are shown in Fig. 3. Note that a different value of the apparent threshold is calculated for each of the MM5280 and C2107 devices.

Petersen, Langworthy, and Diehl[2] propose two SEU figures of merit, one for upsets due to cosmic rays and another for upsets due to protons. They adopt the method of Ref. 1 and this report, with parameter A as the *proton SEU figure of merit*.

Complex Devices

The method given here can be applied for complex circuits as well as for memories. The device SEU cross section is measured using a test program similar to the actual programs. The cross section per bit is taken to be the measured cross section divided by the estimated number of registers involved. The value of A is then calculated with Eq. (3). When calculating device upsets at other proton energies, this approach is insensitive to an error in the number of registers assumed as the curves of Fig. 2 are nearly parallel.

Proton Flux Inside Spacecraft

The average proton flux in earth orbits is tabulated in NASA reports by Stassinopoulos.[12-15] The flux varies with position in orbit, often by many orders of magnitude; see Fig. 4 of Ref. 9. As the path over the rotating earth changes, the flux integrated over an orbit period also varies. Although only the average is treated here, it is necessary, in addition, that a spacecraft be able to handle the peak upset rate.

In reaching a point within a spacecraft, protons are degraded by the material traversed. The energy loss may be computed using proton range-energy tables such as those by Janni.[16]

Langworthy[17] has calculated the mass distribution shielding a device at a "typical" location in a light (<500 lb) spacecraft. The distribution was shown and used by Petersen.[7] The present

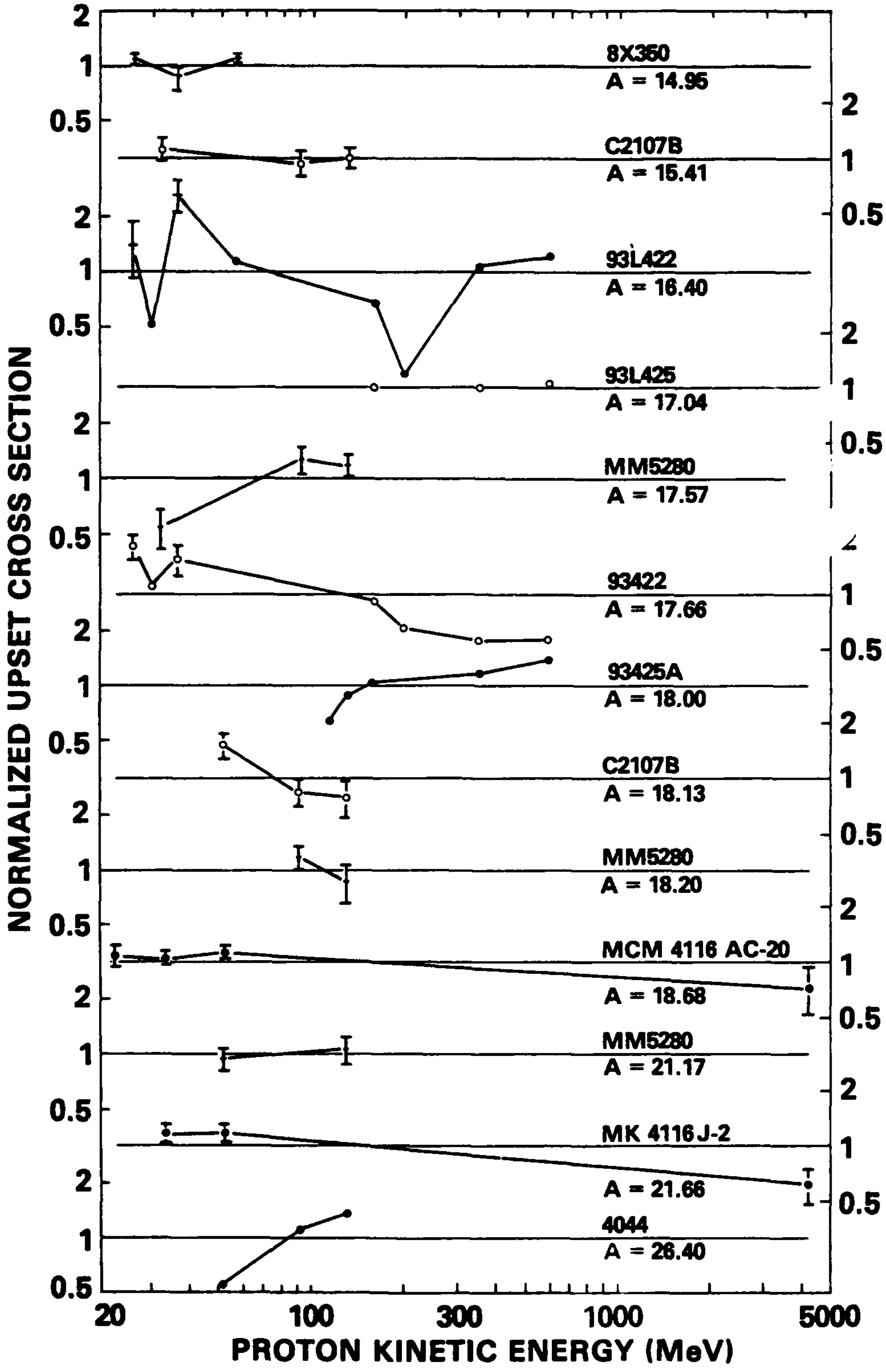

Fig. 3. Ratios of measured SEU cross sections to the values from Eq. (3) with the value of A (MeV) shown.

work employs more bins to fit Langworthy's shield, with 6% of the solid angle at each of

0.72, 0.79, 0.92, 1.12, 1.51,
2.71, 3.45, 4.73, 5.98, 7.55,
10.78, 14.53, 18.53, and 24.12 g/cm^2 Al,

plus 4% each at

29.97, 35.71, 42.58, and 50.85 g/cm^2 Al.

The resultant matrix for distribution of protons from external to internal energy bins is incorporated in the computer program in the appendix. As many protons are stopped before the device is reached, the residual proton spectrum is normally much "harder" than the initial spectrum; see Fig. 2 of Ref. 9.

The results in this report are representative values. The reader may wish to calculate the actual shielding distribution at a typical location in a given spacecraft, or the shielding around a specific device.

Upset Rates

When the internal proton flux for a given orbit is folded with the cross sections of Eq. (3) for given A, the upset rate is obtained. Let us consider a case (the case in the appendix with A = 18 MeV) in which the 80- to 100-MeV bin contains 0.232 X 10^{6} protons/cm^2 per day. The cross section, Eq. (3), averages about 20.9 X 10^{-12} upset per proton/cm^2 per bit. The product is 4.85 X 10^{-6} upsets per bit-day for this bin only. When the products for all bins are summed, the rate is 5.73 X 10^{-5}, in the same units.

Stassinopoulos and Barth[12] present tables of mean proton (and electron) integral fluxes as a function of energy for 60 low-altitude circular orbit environments. Fluxes are given, for solar minimum and for solar maximum, at five altitudes and six orbit inclinations - the angle between the plane of the orbit and the plane of the earth's equator. These fluxes may be distributed to internal differential flux bins, using the "typical" shielding introduced above. The upset rate is then calculated for various values of A. Results, for six values of A from 12 to 30 MeV, are listed in Table 1 for solar minimum and in Table 2 for solar maximum.

Table 3 lists mean upset rate results for 11 other orbits. The first six cases[13] show rate versus altitude at an inclination of 60°. The group of three[14] is at fixed orbit but varying time and solar conditions. (The time specifies the geomagnetic field used in the computation.) The final two[15] cases are non-circular orbits; they are proposed inclinations for the Combined Release and Radiation Effects Satellite (CRRES) orbit.

As seen from Fig. 3, upset rates are determined with limited accuracy. Both the reproducibility of devices and consistency of upset data as a function of energy leave much to be desired. "A basic uncertainty factor of 2" is stated[12] for the proton flux. In addition, the shielding pattern will vary from point to point, even in the same spacecraft. The upset rates *versus A* are thus

Table 1. Single Event Upset rates at SOLAR MINIMUM, as a function of A (MeV) and at a typical location in a light spacecraft in a circular earth orbit. Time = 1980.0. The table entries are in exponent form: 2.86-4 = 2.86 X 10^{-4}. The quantity B appears in Eqs. (4) and (5).

Orbit Incli-nation	A=12	A=15	A=18	A=22	A=26	A=30	B (MeV)
			Upsets per Bit-Day				
Altitude = 200 km = 108 nmi; Period = 1.475 hr							
30°	2.86-4	1.15-5	8.20-7	4.44-8	3.88-9	4.77-10	17.5
35°	7.65-4	3.02-5	2.13-6	1.14-7	9.76-9	1.18-9	12.3
40°	9.58-4	3.77-5	2.65-6	1.40-7	1.20-8	1.45-9	11.2
50°	6.16-4	2.40-5	1.68-6	8.82-8	7.50-9	8.96-10	9.3
60°	4.48-4	1.75-5	1.23-6	6.50-8	5.56-9	6.68-10	10.5
90°	3.72-4	1.46-5	1.02-6	5.41-8	4.62-9	5.55-10	10.5
Altitude = 400 km = 216 nmi; Period = 1.543 hr							
30°	1.17-2	4.75-4	3.43-5	1.88-6	1.66-7	2.06-8	22.1
35°	1.51-2	6.10-4	4.39-5	2.40-6	2.12-7	2.62-8	20.7
40°	1.38-2	5.53-4	3.97-5	2.16-6	1.90-7	2.34-8	19.0
50°	8.72-3	3.49-4	2.50-5	1.36-6	1.19-7	1.47-8	18.2
60°	7.67-3	3.09-4	2.22-5	1.21-6	1.06-7	1.31-8	19.5
90°	5.77-3	2.32-4	1.66-5	9.08-7	7.98-8	9.86-9	19.6
Altitude = 600 km = 324 nmi; Period = 1.611 hr							
30°	6.14-2	2.49-3	1.80-4	9.92-6	8.80-7	1.10-7	23.9
35°	6.20-2	2.51-3	1.81-4	9.93-6	8.79-7	1.09-7	22.3
40°	5.40-2	2.18-3	1.57-4	8.61-6	7.60-7	9.44-8	21.7
50°	3.82-2	1.54-3	1.11-4	6.09-6	5.37-7	6.67-8	21.4
60°	3.13-2	1.27-3	9.13-5	5.00-6	4.42-7	5.49-8	21.8
90°	2.74-2	1.11-3	7.99-5	4.38-6	3.88-7	4.82-8	22.3
Altitude = 800 km = 432 nmi; Period = 1.681 hr							
30°	0.172	6.96-3	5.04-4	2.78-5	2.47-6	3.08-7	24.6
35°	0.160	6.49-3	4.69-4	2.58-5	2.29-6	2.85-7	23.5
40°	0.140	5.67-3	4.09-4	2.25-5	1.99-6	2.48-7	23.0
50°	0.104	4.20-3	3.03-4	1.67-5	1.48-6	1.84-7	23.1
60°	0.0867	3.51-3	2.54-4	1.40-5	1.24-6	1.54-7	23.6
90°	0.0729	2.96-3	2.14-4	1.18-5	1.04-6	1.30-7	23.8
Altitude = 1200 km = 648 nmi; Period = 1.824 hr							
30°	0.709	2.87-2	2.08-3	1.15-4	1.02-5	1.27-6	24.1
35°	0.626	2.54-2	1.84-3	1.01-4	8.96-6	1.12-6	23.7
40°	0.538	2.18-2	1.58-3	8.67-5	7.69-6	9.57-7	23.4
50°	0.420	1.70-2	1.23-3	6.77-5	6.00-6	7.48-7	23.6
60°	0.360	1.46-2	1.06-3	5.81-5	5.15-6	6.42-7	23.9
90°	0.305	1.24-2	8.95-4	4.93-5	4.37-6	5.45-7	24.0

Table 2. Single Event Upset rates at SOLAR MAXIMUM, as a function of A (MeV) and at a typical location in a light spacecraft in a circular earth orbit. Time = 1980.0. The table entries are in exponent form: 5.24-6 = 5.24 X 10^{-6}. The quantity B appears in Eqs. (4) and (5).

Orbit Incli-nation	Upsets per Bit-Day						B
	A=12	A=15	A=18	A=22	A=26	A=30	(MeV)
Altitude = 200 km = 108 nmi; Period = 1.475 hr							
30°	5.24-6	2.16-7	1.58-8	8.82-10	7.92-11	9.98-12	32.1
35°	6.49-5	2.59-6	1.84-7	9.93-9	8.62-10	1.05-10	15.4
40°	1.94-4	7.67-6	5.42-7	2.90-8	2.49-9	3.02-10	12.9
50°	1.14-4	4.49-6	3.17-7	1.69-8	1.45-9	1.75-10	12.4
60°	8.57-5	3.40-6	2.40-7	1.29-8	1.11-9	1.35-10	13.5
90°	6.46-5	2.55-6	1.80-7	9.62-9	8.28-10	1.00-10	12.7
Altitude = 400 km = 216 nmi; Period = 1.543 hr							
30°	5.65-3	2.30-4	1.68-5	9.29-7	8.29-8	1.04-8	27.5
35°	7.78-3	3.16-4	2.28-5	1.26-6	1.11-7	1.39-8	23.5
40°	7.30-3	2.95-4	2.13-5	1.17-6	1.03-7	1.28-8	22.0
50°	4.63-3	1.87-4	1.35-5	7.38-7	6.51-8	8.08-9	21.4
60°	3.98-3	1.61-4	1.16-5	6.36-7	5.62-8	6.98-9	22.0
90°	2.94-3	1.19-4	8.58-6	4.71-7	4.16-8	5.17-9	22.3
Altitude = 600 km = 324 nmi; Period = 1.611 hr							
30°	3.83-2	1.56-3	1.13-4	6.25-6	5.56-7	6.95-8	25.6
35°	3.90-2	1.58-3	1.15-4	6.30-6	5.59-7	6.96-8	23.7
40°	3.52-2	1.42-3	1.03-4	5.64-6	4.99-7	6.21-8	22.7
50°	2.43-2	9.84-4	7.11-5	3.90-6	3.45-7	4.29-8	22.6
60°	1.96-2	7.93-4	5.73-5	3.15-6	2.79-7	3.47-8	23.1
90°	1.74-2	7.05-4	5.10-5	2.80-6	2.48-7	3.09-8	23.4
Altitude = 800 km = 432 nmi; Period = 1.681 hr							
30°	0.122	4.95-3	3.59-4	1.98-5	1.76-6	2.20-7	25.4
35°	0.113	4.60-3	3.33-4	1.84-5	1.63-6	2.03-7	24.5
40°	0.0986	4.00-3	2.89-4	1.59-5	1.41-6	1.76-7	23.8
50°	0.0728	2.95-3	2.13-4	1.17-5	1.04-6	1.30-7	23.8
60°	0.0605	2.45-3	1.78-4	9.79-6	8.69-7	1.08-7	24.5
90°	0.0508	2.06-3	1.49-4	8.23-6	7.31-7	9.13-8	24.8
Altitude = 1200 km = 648 nmi; Period = 1.824 hr							
30°	0.550	2.23-2	1.62-3	8.90-5	7.90-6	9.87-7	24.5
35°	0.487	1.98-2	1.43-3	7.87-5	6.98-6	8.71-7	24.1
40°	0.422	1.71-2	1.24-3	6.80-5	6.03-6	7.52-7	23.8
50°	0.326	1.32-2	9.56-4	5.26-5	4.67-6	5.82-7	24.0
60°	0.278	1.13-2	8.17-4	4.50-5	3.99-6	4.98-7	24.3
90°	0.236	9.57-3	6.93-4	3.82-5	3.39-6	4.23-7	24.4

Table 3. Single Event Upset rates as a function of A (MeV) and at a typical location in a light spacecraft in an earth orbit. The table entries are in exponent form: 4.20-2 = 4.20 X 10^{-2}. B is used in Eq. (5).

Orbit Incli- nation	Upsets per Bit-Day A=12	A=15	A=18	A=22	A=26	A=30	B (MeV)
Solar Maximum; Time = 1989.5							
Altitude = 1667 km = 900 nmi; Period = 1.995 hr							
60°	1.04	4.20-2	3.03-3	1.67-4	1.47-5	1.83-6	22.6
Altitude = 2593 km = 1400 nmi; Period = 2.349 hr							
60°	2.33	9.34-2	6.69-3	3.64-4	3.20-5	3.95-6	19.1
Altitude = 3889 km = 2100 nmi; Period = 2.876 hr							
60°	1.16	4.53-2	3.18-3	1.69-4	1.45-5	1.76-6	11.5
Altitude = 5186 km = 2800 nmi; Period = 3.438 hr							
60°	0.318	1.20-2	8.19-4	4.20-5	3.50-6	4.14-7	5.0
Altitude = 6389 km = 3450 nmi; Period = 3.988 hr							
60°	8.82-2	3.20-3	2.10-4	1.03-5	8.28-7	9.45-8	(0.0)
Altitude = 10,371 km = 5600 nmi; Period = 5.992 hr							
60°	7.87-4	2.42-5	1.36-6	5.39-8	3.53-9	3.33-10	
Altitude = 1111 km = 600 nmi; Period = 1.792 hr							
Solar Max; Time = 1981.8							
63°	0.194	7.86-3	5.69-4	3.14-5	2.78-6	3.48-7	24.4
Solar Min; Time = 1985.8							
63°	0.270	1.09-2	7.91-4	4.35-5	3.86-6	4.81-7	23.9
Solar Max; Time = 1989.0							
63°	0.224	9.11-3	6.59-4	3.63-5	3.22-6	4.02-7	24.2
CRRES: 360 to 36000 km; 194 to 19438 nmi; Period = 10.639 hr							
Solar Minimum; Time = 1985.0							
11°	0.274	1.09-2	7.77-4	4.20-5	3.67-6	4.51-7	16.5
21°	0.147	5.85-3	4.16-4	2.25-5	1.96-6	2.41-7	16.2

uncertain by more than a factor of 2. The SEU rates for devices are even less well known. Relative values are more accurate. The results are sufficient for many purposes, but the limitations must be kept in mind.

The upset rates of Table 1 or 2 are values at points in the three-dimensional space of inclination, altitude, and apparent threshold. Most devices and orbits will not have the values in the table. In order to determine the upset rate in the general case, one must interpolate in all three variables. Interpolation in A will be found to be simple and accurate. Interpolation in orbit, particularly altitude, will be less accurate.

Upset Rate versus A

A plot of upset rate, U, versus A from 12 to 30 MeV, requires

6- or 7-cycle graph paper and cannot be read accurately. The primary cause is the $(24/A)^{14}$ factor in Eq. (3). Without it, the variation would be about a factor of 1.5 (see the printout in the appendix) and a graph could be read much more accurately.

A function which is sufficiently constant would eliminate the need of a U versus A graph. This is a necessary procedure for untabulated orbits - considered below - where U is mapped only for A = 18 MeV. For the orbit "constant", we adopt

$$C = A^{14}\ U\ (A + B). \qquad (4)$$

With U(18) as the input datum, this approximation formula yields

$$U(A)/U(18) = (18/A)^{14}\ (18 + B)/(A + B). \qquad (5)$$

The value of B, chosen to minimize the variation of C from C(18) for the orbit considered, is given in the last column of Tables 1-3. The formula is surprisingly accurate in the region where interpolation of U versus orbit coordinates is most accurate, and is quite satisfactory except at the highest altitude of Table 3. [The error in Eq. (5), for integer A of 12 to 30, is <0.18% at 600 to 2593 km, <0.24% for CRRES, <0.43% at 400 km, and <2.0% at 200 to 5186 km.] The dependence of U upon B is small, thus the interpolation of B between orbits can be done quite crudely; note the big change in B between 30° and 35° orbits at 600 km (Table 1 or 2) and the small difference in the slope of U.

SEU Rate Plots

The calculated upset rates in 60° orbits are shown for solar max in Fig. 4, as a function of altitude and A. Data below 800 nmi are for year 1980; data above are for 1989.5. The upset rate is small at both low and high altitude, reaching a maximum near 1400 nmi (2593 km). Also shown are the rates at 1400 nmi for the devices of Figs. 1 and 3. For A = 18 MeV and this altitude, the upset rate is 0.0067 SEU per bit-day. Of these upsets, only 4.4% are caused by protons having internal energy of 50 MeV or less.

The proportion of upsets produced by various parts of the proton spectrum will vary with A and orbit. Let us assume 80 MeV as the boundary between short-range and penetrating parts of the external proton flux. For the cases of Fig. 4 at A = 18, the external protons with less than 80 MeV energy produce 6 to 10 percent of the upsets at 108 to 1400 nmi - and most of these are due to the 60-80 MeV bin. It is evident that moderate shielding changes will have modest effect in this environment.

For the higher altitude cases, this portion increases to 15, 24, 36, and finally 82 percent at 5600 nmi. Additional shielding will be effective against proton-induced SEUs at high altitude, but shielding is not the route to complete elimination of SEUs. The range of 80 MeV protons is 6.68 g/cm^2 of aluminum.[16] If the spacecraft has an area of 5 square meters, additional shielding of 6 g/cm^2 to stop all protons of <80 MeV would add 660 lb to the

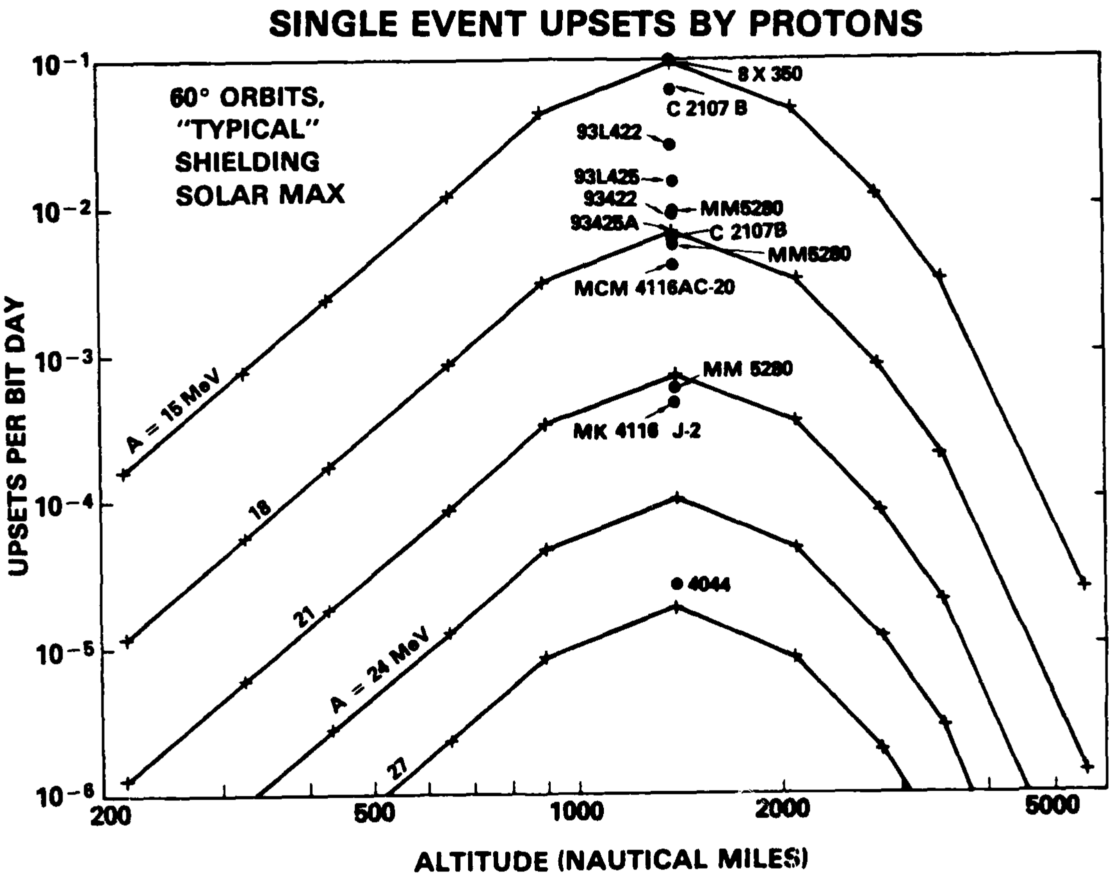

Fig. 4 Upset rates versus altitude and apparent threshold. The environment is that for typical shielding and solar maximum, in circular orbits at 60°. The rates for devices at 1400 nmi use the values of A from the data of Fig. (1) and shown in Fig. (3).

spacecraft mass. Protons of higher energy would still produce upsets.

SEU rates for A = 18 MeV are shown in various ways for the orbits of Tables 1 and 2. These orbits are all below the peak of the proton belts. Figs. 5 and 6, therefore, show that the upset rate increases with altitude at all inclinations. The lines are only slighty curved on these log-log plots, except for the 200 km points at low inclination.

Figure 7 shows that the variation of upset rate with orbit angle is rather small. At the lower altitudes, there is a peak at intermediate inclination; at the higher altitudes, the rate increases as the orbit becomes more equatorial. In all cases, the upset rate is higher at solar minimum, markedly so at 200 km.

It must be emphasized that single event upsets will also be produced by cosmic rays. The intense ionization along the path of a highly-ionized atom allows upset without a nuclear reaction. For many orbits, cosmic rays will be the major source of upsets. The CRRES orbit, with altitude limits of 360 and 36,000 km, will permit investigations over a wide range of space environments. Single event upsets by protons should occur primarily when the satellite traverses the heart of the radiation belt. For protons only, the peak SEU rate for the 21° CRRES orbit is expected to be about 60 times the average rate.

The Solar Max Mission satellite had an orbit at 278 nmi and 29°. Interpolating in Table 2, 13.5 upsets are calculated for a 1024-bit 93422 device in 6 months. Stewart[18] reports that 10 upsets occurred under these conditions, in remarkably good agreement with our prediction. These upsets are attributed to protons because they are seen only when traversing the proton belts at the South Atlantic Anomaly.

Interpolation in Circular Orbits

Figures 5-7, which cover a range of 5.6 cycles in U, can be improved upon for use in interpolation. What is actually graphed is log U, and it is seen to be rather linear with log H, where H is the altitude in km. As many of the points of Fig. 7 are on nearly-parallel lines, adding a term similar to log H will yield a function more suited for interpolation.

We want to reduce the range of the function, but not make the lines overlap, preferably not even cross. A 1.1-cycle graph is adequate when the function

$$W_{min} = \log U + 0.75 \sin(\text{Inclination}) - 2.77 \log [(H-55)/745] \qquad (6)$$

is plotted for solar minimum in Fig. 8. For solar maximum, we define and plot the related function

$$W_{max} = W_{min} + 102/H. \qquad (7)$$

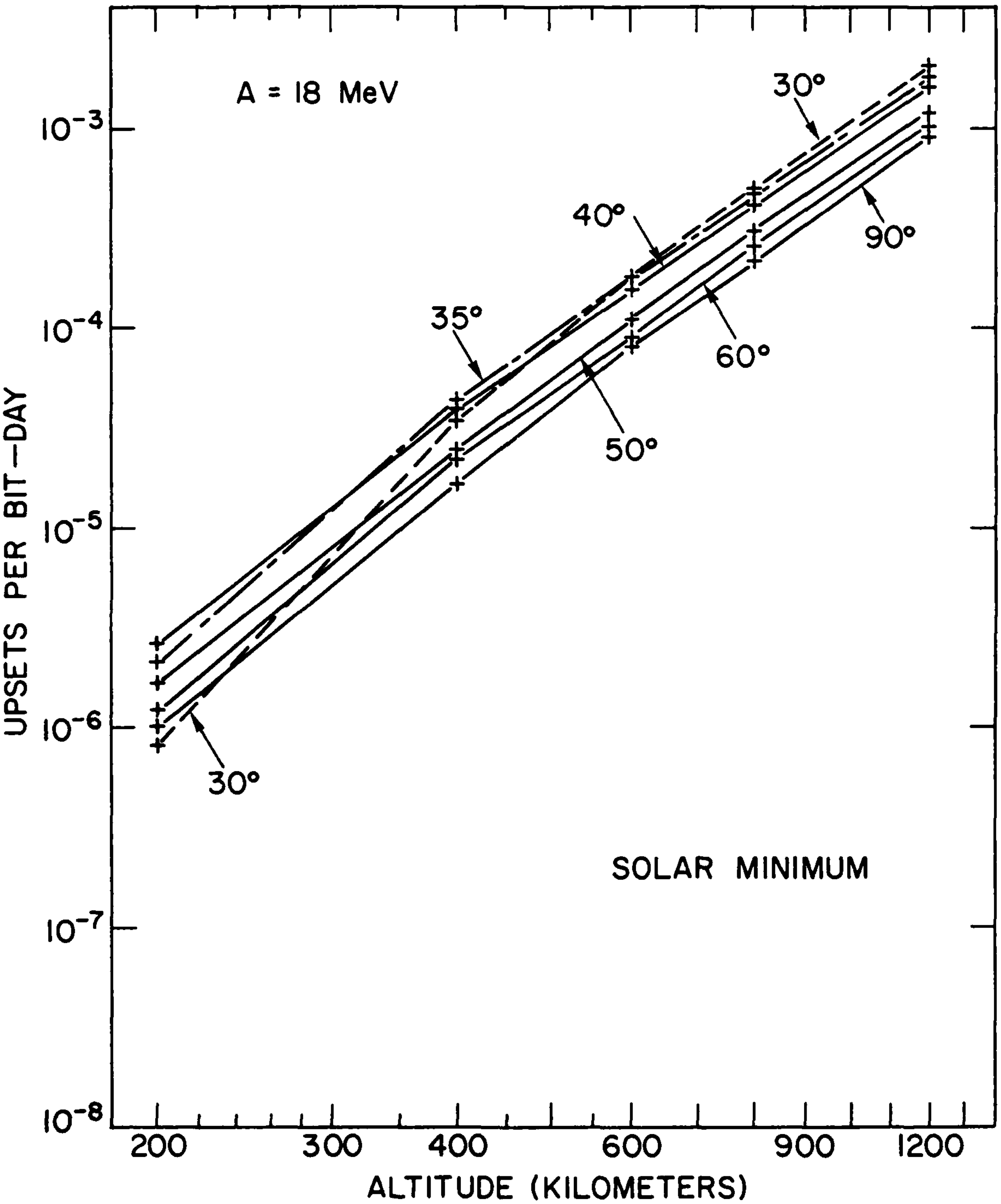

Fig. 5 Predicted solar minimum SEU rates versus altitude, for shielded devices. The points are the thirty A = 18 MeV values from Table 1.

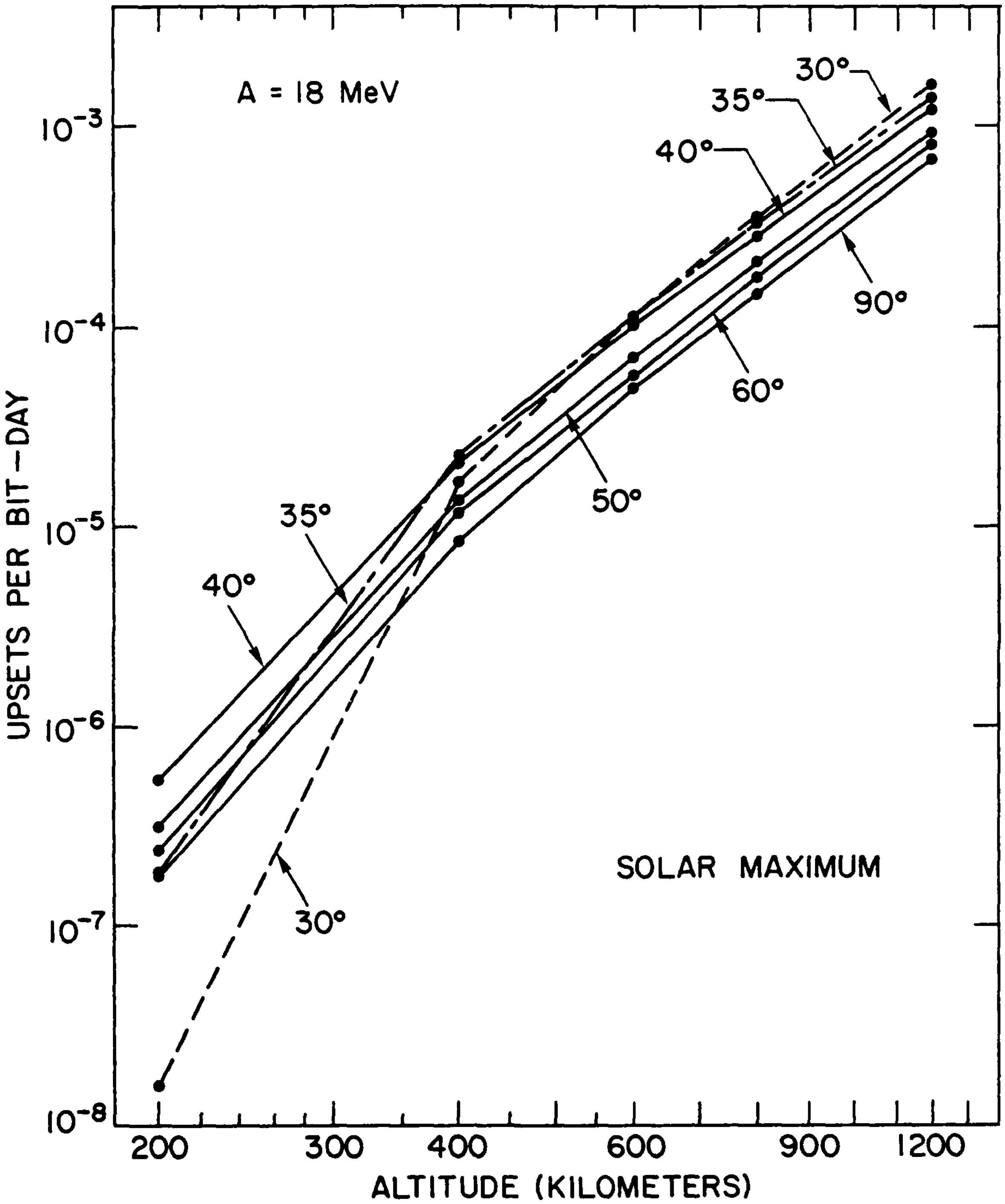

Fig. 6 Predicted solar maximum SEU rates versus altitude, for shielded devices. The points are the thirty A = 18 MeV values from Table 2.

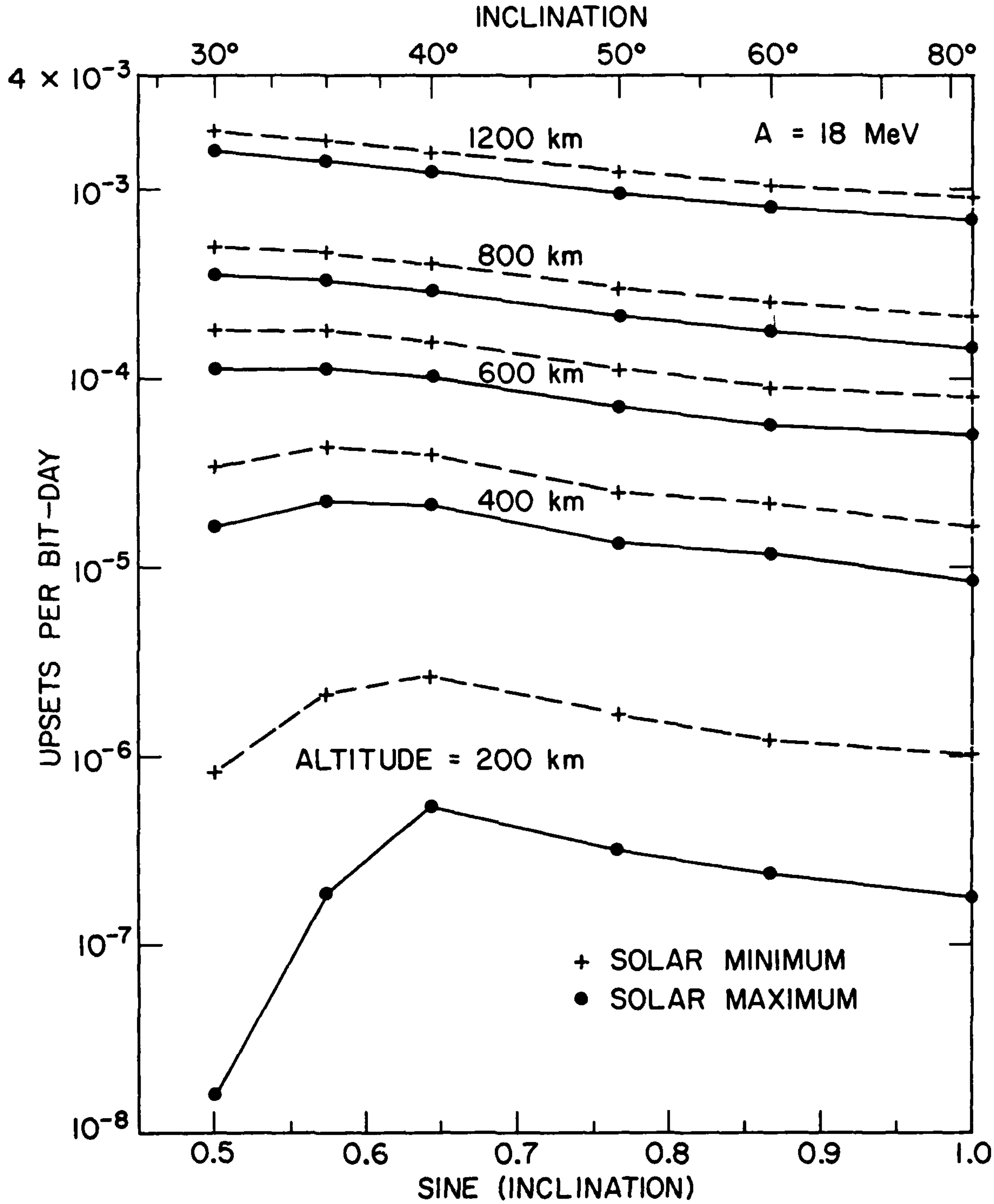

Fig. 7 Predicted SEU rates versus orbit angle, for shielded devices. The sixty A = 18 MeV values from Tables 1 and 2 are used.

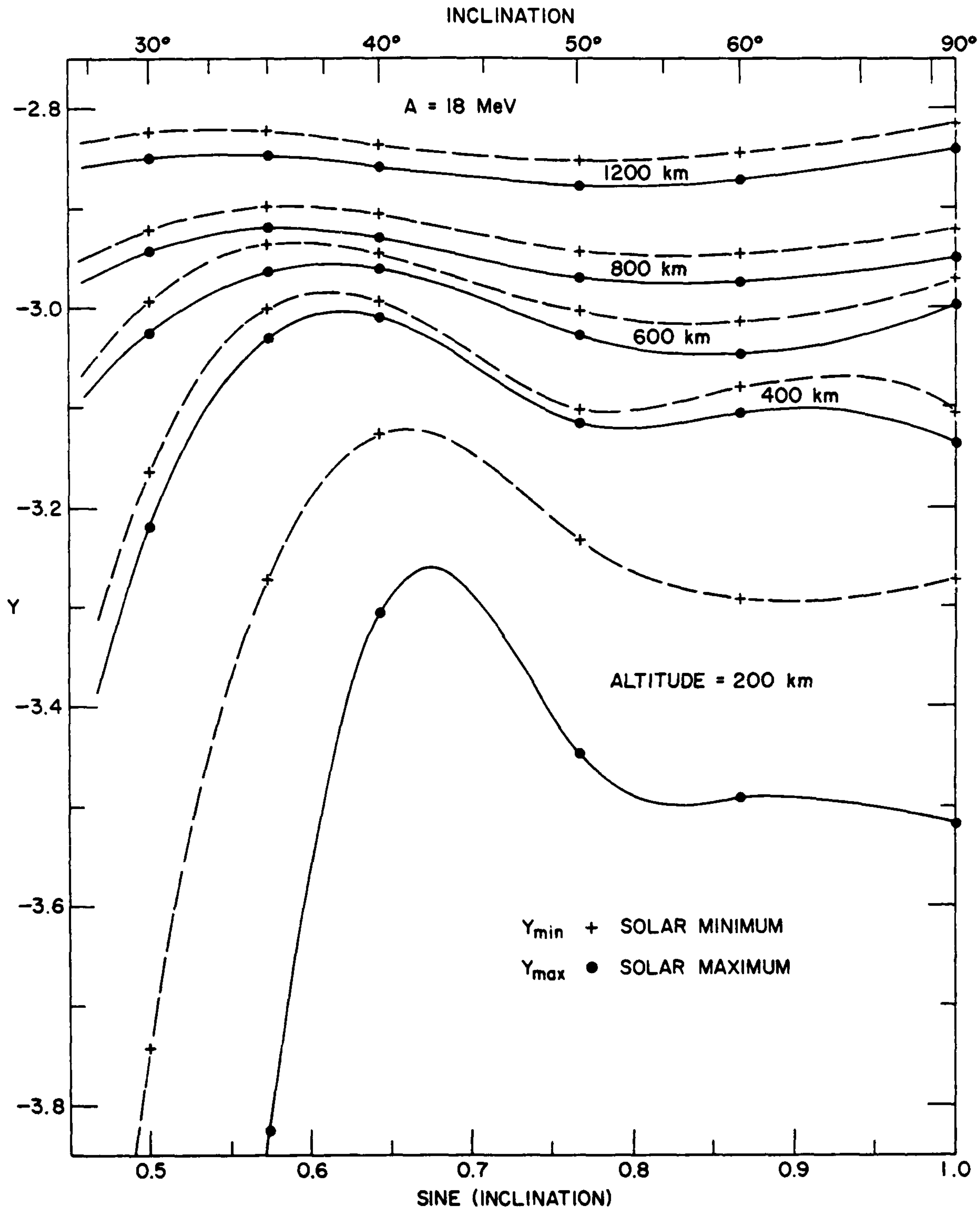

Fig. 8 Graph for SEU rate interpolation; logarithmic functions versus orbit angle, for shielded devices, A = 18 MeV.

Except at 200 km, the two sets of data track very well with a difference of about 0.025. The figure suggests that the accuracy of interpolation in altitude (not to be confused with accuracy of the input data) is rather good above 400 km, and rather poor at lesser altitude. [The curves represent a cubic spline fit to the quantity $-1/(1.6+W)$ at the 6 angles, then evaluated at 15 others. Some of the 200 km, solar max, points are altered up to .007 as a compromise with other types of fits.]

For values of A other than 18 MeV, one first finds log U(18) from Fig. 8 and Eq. (6) or (7), then uses Eq. (5).

SEU Contour Maps

The upset rate may also be presented for circular orbits as a contour map in the sine(inclination), altitude plane. This is done, again using the A = 18 MeV upset rates (Tables 1 and 2) calculated from the orbital flux tables of Stassinopoulos and Barth[12]. The Solar Minimum case is Fig. 9, and Solar Maximum is Fig. 10. These maps seem to illustrate the relative SEU rates expected in this altitude range better than Figs. 5-7, and allow quite accurate interpolation more easily than with Fig. 8.

The contours above 400 km are readily interpolated from the computed points, but those at lower altitude are often uncertain, notably for solar maximum and at small orbit inclination. [The high-altitude W's at each of 21 angles (spline fit, above) define the cubic in log (H/800) used for W above 400 km. A term in the square of log(H/400) is added below 400 km and fitted at 200 km.]

Figures 9 and 10 permit a simple, and reasonably accurate, way of obtaining the upset rate at any value of the parameter A. After reading an upset rate for A = 18 MeV from the appropriate map, employ Eq. (5) to obtain the rate at the desired value of A. It is necessary to find B from Table 1 or 2, but a rough interpolation is adequate.

The CRRES satellite is to be in a highly-elliptical, rather equatorial orbit, with proton environment about equal to that of a circular orbit at 1000 km altitude. Let us compare it with a 1980, 60°, solar minimum orbit using Fig. 8 or 9. The predicted upset rate for CRRES at A = 18 MeV is equal to that at about 920 km for the 21° orbit and 1100 km for the 11° case.

Summary

This report presents a method of predicting proton-induced SEU rates in spacecraft and elsewhere. The method, introduced in Ref. 1, is then used to tabulate and graph results for 71 orbits. Methods of interpolating SEU rates between orbits are presented.

Experimental upset data are obtained at one or more energies, usually with a cyclotron. These data determine the parameter A of Eq. (3) and, therefore, the cross section at all energies. When the proton environment (including the effect of shielding)

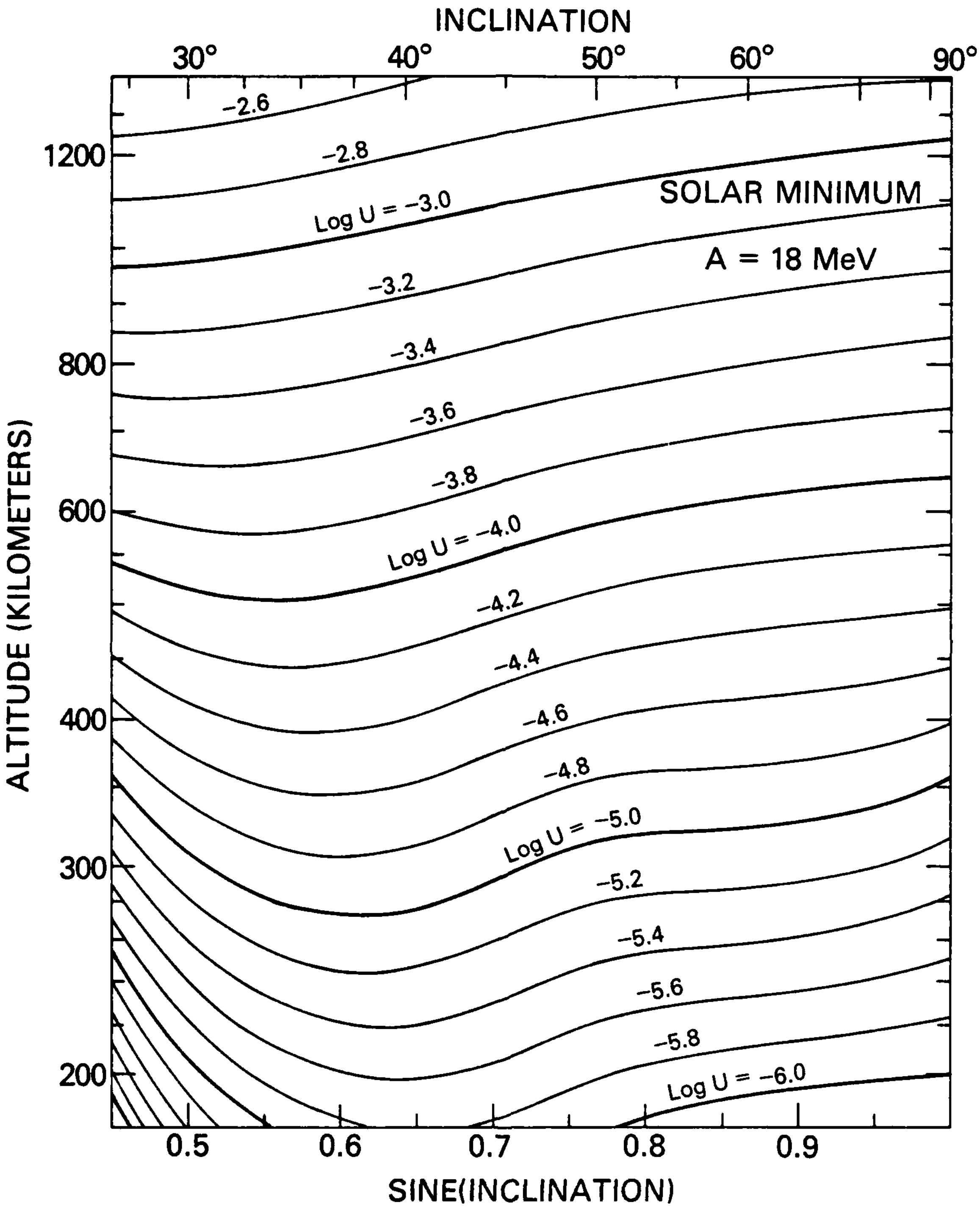

Fig. 9 SEU contour map for circular orbits at solar minimum and A = 18 MeV. The rate, U, is in units of upsets per bit-day.

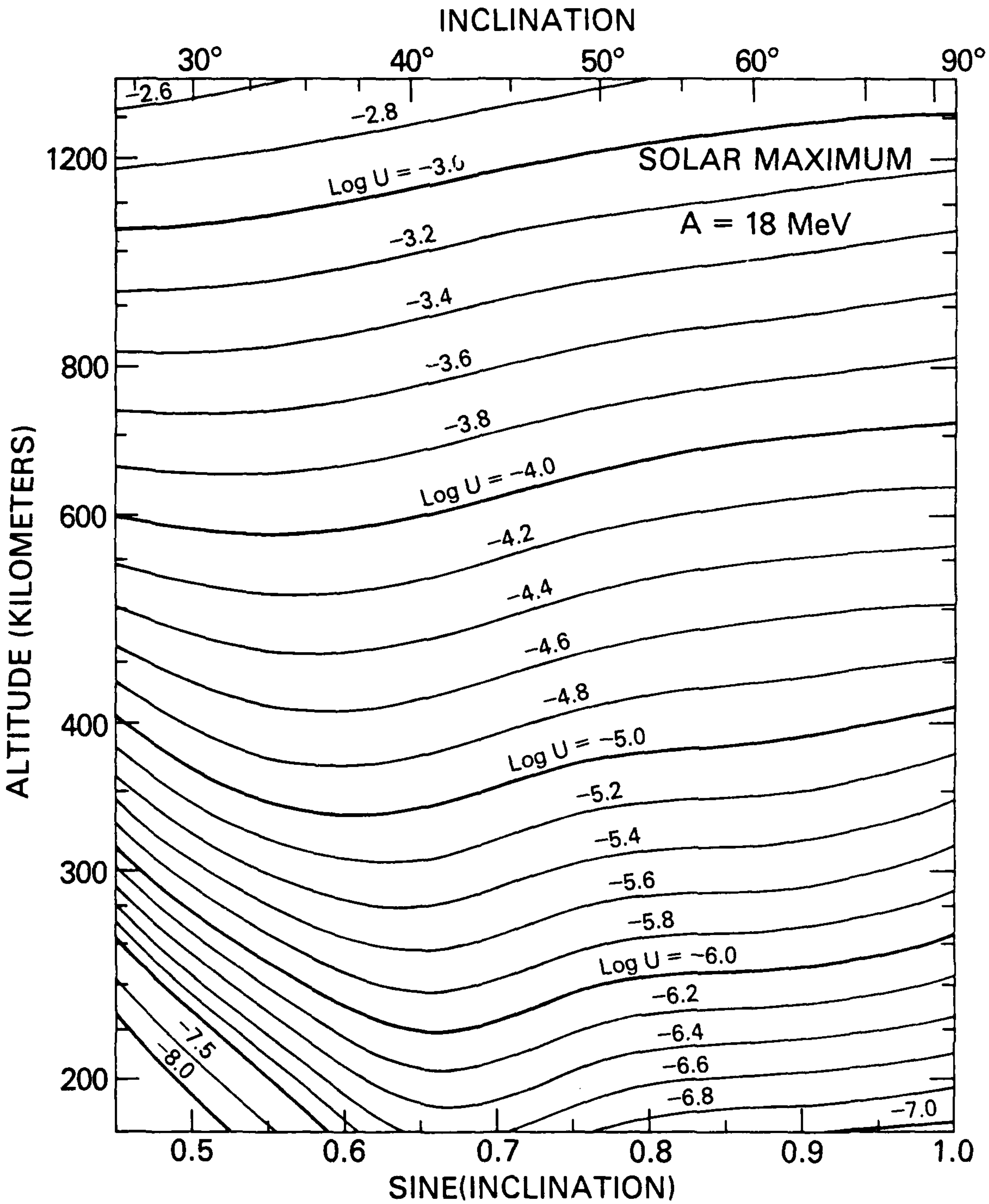

Fig. 10 SEU contour map for circular orbits at solar maximum and A = 18 MeV. The rate, U, is in units of upsets per bit-day.

is specified, the single event upset rate may be computed for a given device -- or tabulated versus the figure of merit, A, as is done here.

The computer program employed, which incorporates the effect of typical shielding in light spacecraft, is listed together with a sample of the input and output data.

Acknowledgments

The work is a continuation, in a little different direction, of studies done by Ed Petersen.[9,10] This report follows Ref. 1, of which he is co-author. Although much material is new, this report necessarily echos much of the earlier text. Clearly, the author is greatly indebted to Dr. Petersen; his ideas and words cannot be expunged from the present report.

Thanks are also due to Jim Ritter and Jim Langworthy for many useful discussions and to C.H. Tsao for pointing out Ref. 11.

References

1. W. L. Bendel and E. L. Petersen, "Proton Upsets in Orbit," IEEE Trans. Nucl. Sci. NS-30, 4481 (1983).

2. E. L. Petersen, J. B. Langworthy, and S.E. Diehl, "Suggested Single Event Upset Figure of Merit," IEEE Trans. Nucl. Sci. NS-30, 4533 (1983).

3. C. S. Guenzer, E. A. Wolicki, and R. G. Allas, "Single Event Upset of Dynamic RAMs by Neutrons and Protons," IEEE Trans. Nucl. Sci. NS-26, 5048 (1979).

4. R. C. Wyatt, et al., "Soft Errors Induced by Energetic Protons," IEEE Trans. Nucl. Sci. NS-26, 4905 (1979).

5. C.S. Guenzer, et al., "Single Event Upsets in RAMs Induced by Protons at 4.2 GeV and Protons and Neutrons Below 100 MeV," IEEE Trans. Nucl. Sci. NS-27, 1485 (1980).

6. P. J. McNulty, et al., "Upset Phenomena Induced by Energetic Protons and Electrons," IEEE Trans. Nucl. Sci. NS-27, 1516 (1980).

7. D. K. Nichols, W. E. Price, and C. J. Malone, "Single Event Upset (SEU) of Semiconductor Devices - A Summary of JPL Test Data," IEEE Trans. Nucl. Sci. NS-30, 4520 (1983).

8. D.K. Nichols, W.E. Price, and J.L. Andrews, "The Dependence of Single Event Upset on Proton Energy (15-590 MeV)", IEEE Trans. Nucl. Sci. NS-29, 2081 (1982).

9. Edward Petersen, "Soft Errors Due to Protons in the Radiation Belt," IEEE Trans. Nucl. Sci. NS-28, 3981 (1981).

10. E. L. Petersen, "Radiation-Induced Soft Fails in Space Electronics," IEEE Trans. Nucl. Sci. NS-30, 1638 (1983).

11. J. R. Letaw, R. Silberberg, and C. H. Tsao, "Proton-Nucleus Total Inelastic Cross Sections: An Empirical Formula for $E > 10$ MeV," Astrop. J. Suppl. 51, 271 (1983).

12. E.G. Stassinopoulos and J.M. Barth, "Non-Equatorial Terrestrial Low Altitude Charged Particle Radiation Environment," NASA-Goddard Space Flight Center report X-601-82-9 (1982).

13. E. G. Stassinopoulos, "Orbital Radiation Study for Inclined Circular Trajectories," NASA-Goddard Space Flight Center report X-601-81-28 (1981).

14. E. G. Stassinopoulos, "The Space Radiation Environment Encountered by a Low-Altitude Geocentric Mission," NASA-Goddard Space Flight Center report X-601-81-7 (1981).

15. E. G. Stassinopoulos and J. M. Barth, "Predicted Charged Particle Environment for the Chemical Release and Radiation Effects Satellite," NASA-Goddard Space Flight Center report X-601-83-1 (1982).

16. Joseph F. Janni, "Proton Range-Energy Tables, 1 keV - 10 GeV," At. Data and Nucl. Data Tables 27, 147-339, 341-529 (1982).

17. James B. Langworthy, private communication (1981).

18. W.N. Stewart, private communication to E.L. Petersen.

Appendix: Computer Program

The early calculations were done without a "computer", but an HP-97 "programmable calculator" was employed. Once the method and equations were developed, an IBM Personal Computer was used to speed calculations on all orbits for which proton spectra were on hand. The IBM Advanced Basic program listed on pages 26 and 27 produced the data of Tables 1-3. The symbols do not agree with those in the main text of this report; parameter A appears as K in the program. Figures in curly brackets, e.g. {500}, are program line numbers.

The proton spectra of Refs. 12-15 were listed on work sheets (top, page 28), together with orbit specifications. These specs are input {400, 410} so that the output (bottom, page 28) may include orbit identification; height in nautical miles {470} and orbit period {500} are incidental calculations. A spectrum is input {420-450} as integral fluxes, F, at 16 minimum energies, from 25 to 500 MeV. A 17th value is generated {560}, and the differential external flux, X, is calculated for 17 energy bins.

The external flux is converted to internal (central) flux, C, in 22 bins {690-760} using a 17x22 matrix {90-270}. The internal bins {320-330} have the same energy spans as the external bins, but bins are added for four groups of slow protons and for the protons stopped before reaching the interior. [A 25-MeV proton, after passing through the minimum shield, has an energy of 8.4 MeV. The input data, therefore, are inadequate if protons under this energy can produce upsets.]

For given apparent threshold A=K {810-830}, the upset rate is calculated {880 up} by summing over bins {1010}, using the cross sections at three points for each bin. If the expected average energy differs {370, 380} from the midbin energy, a correction is made {1000}.

For computation of only those upsets due to protons under 80 MeV, {621} X(J) = 0 and {622} IF J>6 GOTO 640 were added.

The variation of U (upsets per bit-day) with the threshold is primarily due to the 14th-power factor in Eq. (3). The result without this factor, Z {1040}, is slowly varying and is printed with U and log U.

11-03-1983

```
10 REM External to Internal Proton Spectrum; Upsets vs. K
20 DEFINT I-N: DEFSNG A-H, O-Z
30 DIM M(21,16), F(16), X(16), C(21) 'Integral flux, Xternal, Center
40 FOR I = 0 TO 21
50    FOR J = 0 TO 16
60      IF I>(J+5), THEN M(I,J) = 0 ELSE READ M(I,J)
70      NEXT J
80    NEXT I
90 DATA 829,755,700,700,700, 612,525,418,356,277, 177, 78,  9,0,0, 0,0
100 DATA 138,59, 40,  0,  0,  21, 13,  7,  5,  6,   3,  2,  1,0,0, 0,0
110 DATA 33, 67, 27,  2,  0,  19,  7,  3,  3,  3,   1,  1,0,0,0,    0,0
120 DATA  0, 50, 15, 14,  0,  10,  4,  2,  1,  2,   1,0,0,0,0,      0,0
130 DATA  0, 69, 90, 36,  0,  16, 16,  7,  5,  5,   2,  2,  1,0,0, 0,0
140 DATA  0,  0,119, 72, 34,  15, 16, 14,  5,  5,   2,  1,  1,0,0, 0,0
150 DATA      0,  9,148, 64,  16, 22, 14,  6,  7,   3,  2,  1,0,0, 0,0
160 DATA          0, 28,154,  36, 28, 15,  6,  5,   5,  3,  1,0,0, 0,0
170 DATA              0, 48, 109, 21, 25,  6,  4,   6,  2,  1,0,0, 0,0
180 DATA                  0, 107, 32, 20, 17,  5,   7,  3,  2,0,0, 0,0
190 DATA 39,149, 54, 21, 22,  12,  9,  2,  0,  0,   0,0
200 DATA     167,226,107, 45,  31, 18, 11,  0,  0,   0,0
210 DATA         195,240, 90,  44, 23, 16,  0,  0,   0,0
220 DATA             222,210,  60, 31, 20,  0,  0,   0,0
230 DATA                 314, 215, 71, 39, 16,  0,   0,0
240 DATA                      431,288,105, 60,  1,   0,0
250 DATA     466,297,110, 50,   0,  0
260 DATA         493,300,112,  22,  0
270 DATA             514,306,  78,  0,   531,237,6, 663,195,  799
280 DIM L(22), D(21) 'LowerLimit, (av MeV of protons) - midbin
290 FOR I = 0 TO 22
300    READ L(I)
310    NEXT I
320 DATA 0,0,14,18,20,  25,30,35,40,45
330 DATA 50,60,80,100,120,  150,200,250,300,350,  400,500,926
340 FOR I = 0 TO 21
350    READ D(I)
360    NEXT I
370 DATA 0,2,0,.04,.04,  -.04,-.06,-.08,-.09,-.05
380 DATA -.14,-.3,-.5,-.4,-.8, -2.4,-2.2,-2.1,-2,-2,  -8,-128
390 PRINT "Key in orbit and 16 integral fluxes"
400 INPUT "Inclination, altitude in km"; BB, KM
410 INPUT "Solar max (9) or min (0), year"; MM, YY
420 PRINT "": INPUT "5 fluxes, 25+ to 45+ MeV"; F(0),F(1),F(2),F(3),F(4)
430 PRINT "": INPUT "4 more, 50+ to 100+ MeV"; F(5), F(6), F(7), F(8)
440 PRINT "": INPUT "5 more, 150+ to 350+ MeV"; F(10),F(11),F(12),F(13),F(14)
450 PRINT "": INPUT "Last 2 fluxes, 400+ and 500+ MeV"; F(15), F(16)
460 LPRINT "Inclination ="; BB; "degrees"
470 NM = KM/1.852
480 LPRINT "Altitude ="; KM; "km ="; NM; "nmi"
490 IF MM = 0, THEN SS$ = "Solar min, Time =" ELSE SS$ = "Solar Max, Time ="
500 VV = (6378.137 + KM)/5076.85: TT = VV ^ 1.5
510 LPRINT SS$;
520 LPRINT USING "#####.#"; YY;
530 LPRINT SPC(11); "Period =";
540 LPRINT USING "###.###"; TT;
550 LPRINT " hours"    'Orbit params take 3 lines
560 F(9) = (F(8)^.6) * (F(10)^.4): X(16) = F(16)
```

```
570 WIDTH "LPT1:", 60
580 FOR J = 0 TO 16
590    LPRINT USING "#####.##### "; F(J);
600    NEXT J
610 LPRINT " end. integral Flux list"
620 FOR J = 0 TO 15
630    X(J) = F(J) - F(J+1)
640    LPRINT USING "#####.##### "; X(J);
645    IF X(J)<0 GOTO 850    'Input error
650    NEXT J
660 LPRINT USING "#####.##### "; X(16);
670 LPRINT " end. Xternal flux bin list": LPRINT CHR$(10);
680 S = 0   'sum of C
690 FOR I = 0 TO 21
700    C(I) = 0
710    FOR J = 0 TO 16
720      C(I) = M(I,J)*X(J) + C(I)
730      NEXT J
740    C(I) = C(I) * .001: S = C(I) + S
750    LPRINT USING "#####.##### "; C(I);
760    NEXT I
770 LPRINT USING "#####.##### "; S;
780 LPRINT "= sum, Central bins"
790 WIDTH "LPT1:", 80
800 LPRINT " A=K U*(K/24)^14       U        Log U";SPC(20);"Upsets/Bit-Day"
810 FOR N = 12 TO 23
820     K = N: GOSUB 880
830     K = N + 12: GOSUB 880
840     NEXT N
850 BEEP: PRINT " "
860 LPRINT CHR$(10) CHR$(10) CHR$(7)
870 GOTO 390
880    Q = 0: W = SQR(18/K)
890    FOR I = 1 TO 21
900      IF K >= L(I+1) GOTO 1020
910      IF K > L(I) GOTO 1090
920      R = D(I)/2: EA = L(I): H = 1
930      EB = (L(I+1) + EA)/2
940      EQ = (EB - EA)*.7745967
950      E = EB: GOSUB 1110
960      T = 1.6*G
970      E = EB + EQ: GOSUB 1110
980      GC = G: T = G + T
990      E = EB - EQ: GOSUB 1110
1000     T = (GC - G)*R/EQ + (G + T)/3.6
1010     Q = T*H*C(I) + Q
1020     NEXT I
1030   LPRINT K;
1040   Z = Q * .000001: U = (24/K)^14 * Z
1050   LPRINT USING "##.####^^^^ "; Z; U;
1060   V = .4342945 * LOG(U)
1070   LPRINT USING "###.###      "; V;
1080   RETURN
1090     R = 0: EA = K: H = (L(I+1)-K)/(L(I+1)-L(I))
1100     GOTO 930              'K within bin
1110 Y = (E - K)*W  'Energy-dependent func subr
1120 P = -.18 * SQR(Y)
1130 G = (1 - EXP(P))^4
1140 RETURN
1150 END  'EXTINTP.UPK
```

Table 155

INTEGRAL FLUX, E (MeV) to infinity

in units of 10^6 protons/cm² per day

Inclination: 60°

Perigee: / Apogee: 600 km

Solar (MAX) or (min)

Year: 1980.0

25 4.013	30 3.794	35 3.605	40 3.429	45 3.264
50 3.110	60 2.809	80 2.305	100 1.904	120
150 1.120	200 .6740	250 .4001	300 .2401	350 .1449
400 .08779	500 .03277	✓ Period: 1.611 hrs		

Table 157

Inclination: 90°

Perigee: / Apogee: 600 km

Solar (MAX) or (min)

25 3.515	30 3.327	35 3.166	40 3.016	45 2.875
50 2.743	60 2.481	80 2.042	100 1.691	120
150 1.00[illegible]	200	250	300	

```
Inclination = 60 degrees
Altitude = 600 km = 324 nmi
Solar Max, Time = 1980.0                 Period =  1.611 hours
    4.01300        3.79400        3.60500        3.42900        3.26400
    3.11000        2.80900        2.30500        1.90400        1.53988
    1.12000        0.67400        0.40010        0.24010        0.14490
    0.08779        0.03277   end, integral Flux list
    0.21900        0.18900        0.17600        0.16500        0.15400
    0.30100        0.50400        0.40100        0.36412        0.41938
    0.44600        0.27390        0.16000        0.09520        0.05711
    0.05502        0.03277   end, Xternal flux bin list

    1.63486        0.07048        0.03849        0.02188        0.05603
    0.06150        0.06455        0.06679        0.06806        0.06391
    0.13351        0.15317        0.23186        0.20746        0.25494
    0.29368        0.13848        0.11505        0.07070        0.04356
    0.04287        0.02518        4.01300 = sum, Central bins
P=K  U*(K/24)^14      U          Log U                 Upsets/Bit-Day
12   1.1945E-06   1.9571E-02   -1.708        24   8.9130E-07   8.9130E-07   -6.050
13   1.1610E-06   6.2029E-03   -2.207        25   8.7268E-07   4.9278E-07   -6.307
14   1.1296E-06   2.1384E-03   -2.670        26   8.5474E-07   2.7872E-07   -6.555
15   1.1000E-06   7.9265E-04   -3.101        27   8.3742E-07   1.6099E-07   -6.793
16   1.0721E-06   3.1297E-04   -3.504        28   8.2070E-07   9.4826E-08   -7.023
17   1.0456E-06   1.3063E-04   -3.884        29   8.0453E-07   5.6876E-08   -7.245
18   1.0205E-06   5.7271E-05   -4.242        30   7.8888E-07   3.4695E-08   -7.460
19   9.9649E-07   2.6235E-05   -4.581        31   7.7373E-07   2.1502E-08   -7.668
20   9.7362E-07   1.2500E-05   -4.903        32   7.5904E-07   1.3525E-08   -7.869
21   9.5174E-07   6.1717E-06   -5.210        33   7.4479E-07   8.6257E-09   -8.064
22   9.3077E-07   3.1469E-06   -5.502        34   7.3095E-07   5.5737E-09   -8.254
23   9.1065E-07   1.6524E-06   -5.782        35   7.1752E-07   3.6462E-09   -8.438
```

DISTRIBUTION LIST

Jacob A. Abraham
Illinois Computer Research, Inc.
603 W. Green
Champaign, IL 61820

Lorenzo J. Abella
Office of the Deputy Asst Secretary
of the Navy (RAST)
Pentagon 5E731
Washington, DC 20350

Mario H. Acuna
NASA
Goddard Space Flight Center
Code 695
Greenbelt, MD 20771

Orville Adams
TRW Incorporated
Defense & Spa. Sys. Group
One Space Park
Redondo Beach, CA 90278

John W. Adolphsen
NASA, GSFC
Code 311.0
Greenbelt, MD 20771

David Alexander
Mission Research Corporation
1720 Randolph Road, SE
Albuquerque, NM 87106

William Alfonte
Kaman-Tempo
2560 Huntington Avenue
Suite 500
Alexandria, VA 22303

John L. Andrews
General Electric Co.
P.O. Box 8555, M1211
Philadelphia, PA 19101

Robert Antinone
BDM Corporation
1801 Randolph Rd, SE
Albuquerque, NM 87106

Itsu Arimura
Boeing Corp.
MS 2R-00 P.O. Box 3999
Seattle, WA 98124

Robert Armistead
ARACOR
1223 E. Arques Avenue
Sunnyvale, CA 94086

Milton S. Ash
TRW Systems
MS: R6/2184, 1 Space Park
Redondo Beach, CA 90402

Joseph Azarewicz
JAYCOR
11011 Torreyana Road
San Diego, CA 92138

Ali Bahraman
Northrop Research & Tech Center
1 Research Park
Palos Verdes, CA 90274

Ronald A. Belt
Honeywell Inc., MS: MN17-2334
Systems & Research Center
2600 Ridgway Parkway
Minneapolis, MN 55413

Warren L. Bendel
Naval Research Laboratory
Code 6611
Washington, DC 20375

Ben Bernstein
NASA Headquarters
Office of the Chief Engineer
Code DP
Washington, DC 20546

Franklyn Blaha
Westinghouse Advanced Technology Lab
MS: 3527 - P.O. Box 1521
Baltimore, MD 21203

Bernard Blake
The Aerospace Corp.
P.O. Box 92957
Los Angeles, CA 90009

James Blandford
Rockwell International
Science Center, P.O. Box 4192
MS/277-063 031-GB17
3370 Miroloma Ave.
Anaheim, CA 92803

Harold E. Boesch, Jr.
Harry Diamond Laboratory
MS: Br. 22300
2800 Powder Mill Road
Adelphi, MD 21045

Edward J. Boling
Westinghouse Electric
MS: 3431
Advanced Tech. Div.
Nursery and Winterson Road
Linthicum, MD 21090

Stewart Bower
Aerospace Corporation
P.O. Box 92957
Los Angeles, CA 90009

John N. Bradford
RADC/ESR
Dept for Electronic Tech.
M/S 64
Hanscom AFB, MA 01731

George J. Brucker
RCA Corporation
David Sarnoff Research Center
MS/TR6-B, P.O. Box 800
201 Washington Road
Princeton, NJ 08540

Robert Buchanan
ATTN: ESR
Rome Air Development Center
Hanscom AFB, MA 01731

Paltiel Buchman
Aerospace Corporation
2350 E. El Segundo Blvd.
El Segundo, CA 90009

Edward A. Burke
RADC/BSRE
Hanscom Air Force Base, MA 01731

Milton L. Buschbom
Texas Instruments
MS: 914, P.O.Box 225621
13500 N. Central Expressway
Dallas, TX 75265

Arthur B. Campbell
Code 6613
Naval Research Laboratory
Washington, DC 20375

Alan Carlan
The Aerospace Corp.
MS/M4 935
P.O. Box 92957
Los Angeles, CA 90009

Richard G. Carroll
Texas Instruments
P.O. Box 660246
Forest Lane, MS: 3145
Dallas, Texas 75266

Tom Cheek
Texas Instrument
MS: 3145, P.O. Box 660246
Dallas TX 75266

John Choma
Univ. of Southern Cal
EE Department
University Park - 0271
Los Angeles, CA 90089

Larry R. Cooper
Code 414
Office of Naval Research
800 N. Quincy Street
Arlington, VA 22217

Floyd Coppage
Sandia Laboratories
P.O. Box 5800, D/4365
Albuquerque, NM 87185

William Crane
Aerospace Corp
M1/047
P.O. Box 92957
Los Angeles, CA 90009

Mr. John Criscuolo
TRW Incorporated
Defense & Space Systems Group
One Space Park, 134-9039
Redondo Beach, CA 90278

Vitaly Danchenko
Code 754
NASA-GSFC
Greenbelt, MD 20771

Edward S. Davidson
Illinois Computer Research Inc.
2114 Lynwood Drive
Champaign, IL 61820

Gracie Davis
Naval Research Laboratory
Code 6816
Washington, DC 20375

William Dawes
Sandia Laboratories
Department 2110
P.O. Box 5800
Albuquerque, NM 87183

Daniel DiCenzo
DESC-ECS
1507 Wilmington Pike
Dayton, OH 45444

Sherra E. Diehl-Nagle
North Carolina State University
Department of Electrical Engineering
P.O. Box 7911
Raleigh, NC 27795

Paul Dressendorfer
Sandia Laboratories
Division 2144
P.O. Box 5800
Albuquerque, NM 87185

Harvey Eisen
DELHD-RBH
Harry Diamond Laboratory
Department of the Army
2800 Powder Mill Rd.
Adelphi, MD 20783

Thomas Ellis
Naval Weapons Support Center
Code 3073, Bldg. 2917
Crane, IN 47522

William H. Evans
Hughes Aircraft Company
Bldg. E 1, F132
P.O. Box 902
El Segundo, CA 90230

James Ferry
Air Force Weapons Laboratory (NTYC)
Kirtland AFB, NM 87117

Robert Filz
AFGL-PLIG
Hanscom AFB, MA 01731

Roger Fitzwilson
Science Applications, Inc.
1200 Prospect Street
P.O. Box 2351
La Jolla, CA 92038

Thomas Frey
Control Data Corporation
2300 E. 88th Street
Minneapolis, MN 55419

Kenneth Galloway
National Bureau of Standards
Technology Bldg., Rm A-305
Washington, DC 20234

George Gilley
The Aerospace Corp.
P.O. Box 92957
Los Angeles, CA 90009

Dennis Grimes
Westinghouse Electric
Radiation Effects Technology
P.O. Box 746, M/S 1627
Baltimore, MD 21203

Harold L. Grubin
Scientific Research Associates
P.O. Box 498
Gastonbury, CN 06033

Leon Hamiter
NASA Marshall Space Flight Center
Code EC43
Huntsville, AL 35812

John Harrity
IRT Corporation
3030 Callan Road
Torrey Pines Science Park
San Diego, CA 92121

Gary Havey
Honeywell SRC
MS: MN17-2334
2600 Ridgway Parkway
Minneapolis, MN 55440

David Haykin, Jr.
Code 710.2, Bldg 22
NASA, GSFC
Greenbelt, MD 20771

Maj. Burl Hickman
Defense Nuclear Agency (RAEV)
6801 Telegraph Road
Alexandria, VA 20310

D. Hoeschele
General Electric Company
P.O. Box 8555
Philadelphia, PA 19101

David Holtkamp
MS: H818
Los Alamos Nat. Laboratory
Los Alamos, NM 87545

Harold Hughes
Naval Research Laboratory
Code 6816
Washington, DC 20375

Lt. Col. Steven Hunter
Space Division
Air Force Systems Comd.
P.O. Box 92960
Worldway Postal Center
Los Angeles, CA 90009

Alan Johnston
Boeing Aerospace Company
MS-2R-00
P.O. Box 3999
Seattle, WA 98124

Capt. Richard Joseph
DST/DNA
MS F635
Los Alamos National Lab
Los Alamos, NM 87545

Vern Josephson
The Aerospace Corp.
MS M-4-933
P.O. Box 93957
Los Angeles, CA 90009

Roger Judge
IRT Corp.
7650 Convoy Ct.
P.O. Box 80817
San Diego, CA 92138

Frank Junga
Lockheed Research Lab.
3251 Hanover Street
52/54-202/2
Palo Alto, CA 94304

Maj. Daniel Kadel
LP
Johnson Space Center
NASA
Houston, TX 77058

Henry Kalapaca
Westinghouse Electric Corporation
Radiation Effects Technology
P.O. Box 16934 M/S 1627
Baltimore, MD 21203

Robert Karpen
Code DP
NASA Headquarters
Washington, DC 20546

Capt Craig Kimberlin
Defense Nuclear Agency (RAEV)
6801 Telegraph Road
Alexandria, VA 20310

Everett King
Northrop Electronics Div.
2301 W. 120th Street (C 3325/N3)
Hawthorne, CA 90250

Jack Kinn
Electronic Industries Assoc.
2001 Eye Street, NW
Washington, DC 20006

Charles Kleiner
Rockwell International
P.O. Box 4192, MS GB 10
3370 Miraloma Avenue
Anaheim, CA 92803

Robert Kloster
McDonnell Douglas Corp.
MS/101A-3-350
St. Louis, MO 63166

Alvin R. Knudson
Naval Research Laboratory
Code 6673
Washington, DC 20375

Wojciech Kolasinski
Aerospace Corporation
Building M2, MS/259
P.O. Box 92957
Los Angeles, CA 90009

Clyde Lane
Rome Air Development Center
RADC/RBRP
Griffiss AFB, NY 13441

James B. Langworthy
Code 6611
Naval Research Laboratory
Washington, DC 20375

B. J. Lee
169-427
Jet Propulsion Laboratory
California Inst. of Tech.
Pasadena, CA 9110

David Long
Science Applications Inc.
1200 Prospect Street
La Jolla, CA 92038

Paul Losleben
DARPA
IPTO
1400 Wilson Blvd.
Arlington, VA 22209

Clarence Lund
B132
Motorola
P.O. Box 2953
Pheonix, AZ 85008

Carl Malone
Jet Propulsion Laboratory
MS/158-205
4800 Oak Grove Drive
Pasadena, CA 91109

Thomas T. Marquitz
Central Intelligence Agency
Washington, DC 20505

Gerald Masson
Dept. of Elec. Engineering
Barton Hall
Johns Hopkins University
Baltimore, MD 21218

Richard Maurer
Johns Hopkins Applied Physics Lab.
Johns Hopkins Road
Laurel, MD 20707

Timothy May
INTEL Corporation
MS WW2-265
3885 S.W. 198th Avenue
Aloha, OR 97077

Jerry Mayland
Honeywell Inc.
12001 State Highway 5
Plymouth, MN 55441

James McGarrity
Harry Diamond Laboratories
DELHD-RB-RC/Br 22300
2800 Powder Mill Rd.
Adelphi, MD 20783

Thomas McGill
California Inst. of Technology
Applied Physics, 28-95
Pasadena, CA 91125

William E. McInnis
Office of the Chief Engineer
Code D
NASA
Washington, DC 20546

Peter J. McNulty
Clarkson University
Physics Department
Potsdam, NY 13676

R. J. McPartland
Bell Laboratories
555 Union Blvd.
Allentown, PA 18103

John Meason
ATTN: STEWS-TE-AN, P.O.Box 215
White Sands Missile Range, NM
88002

George C. Messenger
Consultant, DNA
3111 Bel Air Drive, 7-F
Las Vegas, NV 89109

Sheldon Meth
The BDM Corporation
7915 Jones Branch Drive
McLean, VA 22102

Douglas Millward
Science Applications, Inc.
1200 Prospect St., MS #1
La Jolla, CA 92038

Cmdr. William Mohr
NAVELEX-PME-106-491
NC-1 RM3W80
2511 Jefferson Davis Highway
Washington, DC 21114

Gary Mullen
AFGL-PHG, M/S 30
Hanscom AFB, MA 01731

John Mullis
AFSC (NTCTR)
Air Force Weapons Laboratory
Kirtland AFB
Albuquerque, NM 87117

Deb Newberry
Control Data Corporation
BRR 142
2300 E. 88th Street
Bloomington, MN 55420

Don Newell
Ford Aerospace
1663 New Brunswick Avenue
Sunnyvale, CA 94087

Donald Nichols
Jet Propulsion Laboratory
T-1180
4800 Oak Grove Drive
Pasadena, CA 91109

David W. Nielsen
Honeywell SSED
MN 14-3005
12001 State Highway 55
Plymouth, MN 55441

J. K. Notthoff
McDonnell Douglas
MS 28-1
5301 Bolsa Avenue
Huntington Beach, CA 92647

Tim O'Gorman
Department E62
Building 966-2
IBM
Burlington, VT 05452

Timothy R. Oldham
Harry Diamond Laboratories/ERADCOM
2800 Powder Mill Road
Adelphi, MD 20783

William Oldham
Electrical Engineering Dept.
University of California
Berkley, CA 94720

Roy Olson
MS AC34
Rocketdyne
6633 Conoga Avenue
Conoga Park, CA 91304

Les Palkuti
ARACOR
1223 E. Argues Avenue
Sunnyvale, CA 94086

David O. Patterson
Naval Research Laboratory
Code 6816
Washington, DC 20375

Joseph Peden
General Electric Co.
Valley Forge Space Center
P.O. Box 8555
Philadelphia, PA 19101

Edward Petersen
Naval Research Laboratory
Code 6611
Washington, DC 20375

Howard Phillips
Electronics Research Laboratory
The Aerospace Corporation
P.O. Box 92957
Los Angeles, CA 90009

James C. Pickel
Rockwell International
MS BA01, Science Center
3370 Miraloma Avenue
Anaheim, CA 92803

Dale Platteter
NWSC Crane
Code 6054, Building 2917
Crane, IN 47522

Frank W. Poblenz
Texas Instruments, Inc.
P.O. Box 226015, MS 3148
Dallas, TX 75266

William E. Price
Jet Propul Lab., MS 83-122
Cal. Inst. Tech. (T-1180)
4800 Oak Grove Drive
Pasadena, CA 91109

Jeffrey S. Pridmore
RCA Corp - Advanced Technology Labs
Building 10-8-1
Front & Cooper Streets
Camden, NJ 08102

James L. Ramsey
Scientific Analysis Branch
NWSC/WQEC
Crane, IN 47522

James P. Raymond
Mission Research Corporation
5434 Ruffin Road
San Diego, CA 92123

William N. Redisch
NASA, GSFC
Code 701
Greenbelt, MD 20771

Phil Reid
MS R6/2541
TRW
1 Space Park
Redondo Beach, CA 90278

Richard B. Reincke
Honeywell Inc.
MS FL51-725-4A
13350 US 19 S
St. Petersburg, FL 33546

John P. Retzler
Nuclear S/V Manager
Litton Guidance & Control
5500 Canoga Avenue, 87/31
Woodland Hills, CA 91367

Richard Reynolds
Dep. Dir., Defense Sci. Off.
Defense Advanced Research
Projects Agency
1400 Wilson Blvd.
Arlington, VA 22209

Jim Ritter
Code 6610
Naval Research Laboratory
Washington, DC 20375

Leonard R. Rockett
IBM Corp., Federal Systems Div.
MS 110-020
9500 Godwin Drive
Manassas, VA 22110

Clay Rogers
JAYCOR
2309 Renard Place, S.E.
Suite 201
Albuquerque, NM 87119

Sven Roosild
Defense Advanced Research
Projects Agency, DSO
1400 Wilson Blvd.
Arlington, VA 22209

Carl Rosenberg
Boeing Aerospace Company
MS-2R-00
P.O. Box 3999
Seattle, WA 98124

Steven Sabin
Texas Instruments
MS: 3143, P.O. Box 226150
Forest Lane
Dallas, TX 75266

G. A. Sai-Halasz
Thomas J. Watson Res. Center
IBM - P.O. Box 218
Yorktown Heights, NY 10598

Howard H. Sander
Sandia Laboratories
Division 2143, P.O. Box 5800
Albuquerque, NM 87185

Harry Schafft
National Bureau of Standards
Code A 327
Washington, DC 20234

Vincent Sferrino
MIT Lincoln Labs
P.O. Box 73
Lexington, MA 02173

Philip Shapiro
Naval Research Laboratory
Code 6614
Washington, DC 20375

Walter Shedd
Rome Air Development Center
ESR
Hanscom AFB, MA 01731

Edward Simon
Unitrode Corporation
580 Pleasant Street
Watertown, MA 02172

Court Skinner
National Semiconductor
MS D3677
2900 Semiconductor Drive
Santa Clara, CA 95051

Mayrant Simons
Research Triangle Institute
P.O. Box 12194
Research Triangle Park, NC
27707

Edward C. Smith
Hughes Aircraft Co
P.O. Box 92919
Bldg. 541, MS/B301
Los Angeles,CA 90009

Edwin A. Smith
Department 6223
Building 538
Lockheed Missiles & Space Co.
P.O. Box 504
Sunnyvale, CA 94086

Lewis Smith
Litton Guidance & Control
MS 76-31
5500 Conoga Avenue
Woodland Hills, CA 91367

James P. Spratt
Science Applications Inc.
2615 Pacific Coast Highway
Hermosa Beach, CA 90254

Joseph R. Srour
Northrop Research & Tech Center
MS/0355/T60
One Research Park
Palos Verdes Peninsula
CA 90274

E. G. Stassinopoulos
NASA-GSFC
Code 601
Greenbelt, MD 20771

C. Martin Stickley
BDM Corporation
7915 Jones Branch Drive
McLean, VA 22102

Allan H. Taber
IBM FSD
110/036
9500 Godwin Drive
Manassas, VA 22110

Norman Tibbetts
MS 11
Charles Draper Labs
555 Technology Square
Cambridge, MA 02145

Fred Tietze
IBM Federal Systems Division
9500 Godwin Drive
Manassas, VA 22110

James H. Trainor
NASA, GSFC
Code 660
Greenbelt, MD 20771

Morris Tsou
National Semiconductor
M/S A1525
2900 Semiconductor Drive
Santa Clara, CA 95051

Patrick J. Vail
RADC/ESR
Hanscom AFB, MA 01731

Victor Van Lint
Defense Nuclear Agency (DDST
6801 Telegraph Road
Alexandria, VA 20305

R. Viola
Sperry Rand Corporation
Sperry Division
Marcus Avenue
Great Neck, NY 11020

Edmund J. Vitek
Westinghouse Electric Corp
MS 3200
P.O. Box 1521
Baltimore, MD 21203

Hubert Volmerange
TRW
R1-1126
One Space Park
Redondo Beach, CA 90278

Steven S. Wharfield
Hughes Aircraft Co.
Bldg 530 M/S P 323
P.O. Box 92919
Los Angeles, CA 90009

Neil Wilkin
Harry Diamond Laboratories
2800 Powder Mill Road
Adelphi, MD 20783

William Willis
TRW Incorporated
Defense & Space Systems Group
1 Space Park
Redondo Beach, CA 90278

Abe Witteles
MS R1/2144
TRW Incorporated
Defense & Space Systems Group
1 Space Park, R1-2144
Redondo Beach, CA 90278

Eligius A. Wolicki
Code 6601
Naval Research Laboratory
Washington, DC 20375

David S. Yaney
Bell Laboratories, Inc.
555 Union Blvd.
Allentown, PA 18103

James Ziegler
IBM
Thomas J. Watson Res. Ctr.
P.O. Box 218
Yorktown Heights, NY 10598

John Zoutendyk
Jet Propulsion Lab + 1180
Cal. Inst. of Technology
MS 158-205
4800 Oak Grove Drive
Pasadena, CA 91109

0690B/0074B (With stops for printing envelopes
0690B/0064B (Without stops for dual column printout)